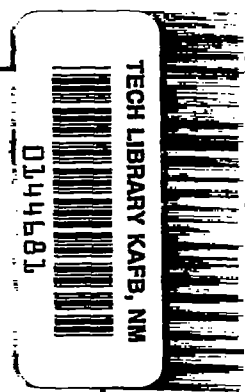


NATIONAL ADVISORY COMMITTEE FOR AERONAUTICS



TECHNICAL MEMORANDUM

No. 1216

AN APPROXIMATE METHOD FOR CALCULATION OF THE LAMINAR BOUNDARY LAYER WITH SUCTION FOR BODIES OF ARBITRARY SHAPE

By H. Schlichting

Translation of "Ein Näherungsverfahren zur Berechnung der
laminaren Grenzschicht mit Absaugung bei beliebiger Körperform"
from Aerodynamisches Institut der Technischen Hochschule
Braunschweig, Bericht 43/13, June 1943



Washington
March 1949

95:11 1949 MAR 1 1949

219 98/12



0144681

NATIONAL ADVISORY COMMITTEE FOR AERONAUTICS

TECHNICAL MEMORANDUM NO. 1216

AN APPROXIMATE METHOD FOR CALCULATION OF THE
LAMINAR BOUNDARY LAYER WITH SUCTION FOR
BODIES OF ARBITRARY SHAPE*

By H. Schlichting

Outline:

- I. Introduction: Statement of the Problem
- II. Symbols
- III. The Boundary Layer Equation with Suction
- IV. The General Approximation Method for Arbitrary Pressure Distribution and Arbitrary Distribution of the Velocity of Suction
 - (a) The expression for the velocity distribution
 - (b) The differential equation for the momentum thickness
 - (c) Stagnation point and separation point
 - (d) Execution of the calculation for the general case
- V. Special Cases
 - A. Without suction
 - (a) The plane plate in longitudinal flow
 - (b) The two-dimensional stagnation point flow
 - B. With suction
 - (a) The growth of the boundary layer for the plane plate in longitudinal flow with homogeneous suction
 - (b) The two-dimensional stagnation point flow with homogeneous suction
- VI. Examples
 - (a) The circular cylinder with homogeneous suction for various suction quantities
 - (b) Symmetrical Joukowsky profile for $c_a = 0$ with homogeneous suction
- VII. Summary
- VIII. Bibliography
- IX. Appendix

*"Ein Näherungsverfahren zur Berechnung der laminaren Grenzschicht mit Absaugung bei beliebiger Körperform." Aerodynamisches Institut der Technischen Hochschule Braunschweig, Bericht 43/13, June 12, 1943.

I. INTRODUCTION

Various ways were tried recently to decrease the friction drag of a body in a flow; they all employ influencing the boundary layer (reference 1). One of them consists in keeping the boundary layer laminar by suction; promising tests have been carried out by Holstein (references 2 and 3) and Ackeret (reference 4). Since for large Reynolds numbers the friction drag of the laminar boundary layer is much lower than that of the turbulent boundary layer, a considerable saving in drag results from keeping the boundary layer laminar, even with the blower power required for suction taken into account. The boundary layer is kept laminar by suction in two ways: first, by reduction of the thickness of the boundary layer and second, by the fact that the suction changes the form of the velocity distribution so that it becomes more stable, in a manner similar to the change by a pressure drop (reference 7). Thereby the critical Reynolds number of the boundary layer $(U_0^*/\nu)_{crit}$ becomes considerably higher than for the case without suction. This latter circumstance takes full effect only if continuous suction is applied which one might visualize realized through a porous wall. Thus the suction quantities required for keeping the boundary layer laminar become so small that the suction must be regarded as a very promising auxiliary means for drag reduction.

Various partial solutions exist at present concerning the theoretical investigation of this problem. Thus H. Schlichting (references 5 and 6) investigated the plane plate in longitudinal flow with homogeneous suction. At large distance from the leading edge of the plate a constant boundary layer thickness and an asymptotic suction profile result. Later H. Schlichting and K. Bussmann (reference 9) investigated the two-dimensional stagnation point flow with homogeneous suction and the plate in longitudinal flow with $v_0 \sim 1/\sqrt{x}$ (x = distance from the leading edge of the plate). In all cases a strong dependence upon the mass coefficient of the suction resulted for the velocity distribution and the other boundary layer quantities. K. Bussmann, H. Münz (reference 8), and A. Ulrich (reference 16) calculated the transition from laminar to turbulent (stability) of the boundary layer with suction for several cases; in all of them the stability limit was found to have been raised considerably by the suction. As is known from earlier investigations (reference 7), the same amount of influence on the transition from laminar to turbulent is exerted by the pressure gradient along the contour in the flow for impermeable wall. Both influences (pressure gradient and suction) will be present simultaneously for the intended maintenance of a laminar boundary layer for a wing. Both influences have a stabilizing effect for the suction in the region of pressure drop; in the region of pressure rise, however, pressure gradient and suction have opposite influences. Whereas without suction, for pressure rise, mostly transition in the boundary

layer occurs; here the important problem arises whether this transition can be suppressed by moderate suction.

The solutions for the laminar boundary layer with suction existing so far are not sufficient for answering these questions. An exact calculation of the boundary layer with suction encounters insuperable numerical difficulties just as in the case of the impermeable wall. Thus it is the more important to have an approximation method at disposal which permits one to check the calculation of the boundary layer with suction for an arbitrary body. Such a method will be developed in the present treatise. The method given here is an analogon to the well-known Pohlhausen method for impermeable wall. It permits the calculation of the laminar boundary layer with suction for an arbitrarily prescribed shape of the body and an arbitrarily prescribed distribution of the suction velocity along the contour in the flow.

I I. S Y M B O L S

(a) Lengths

x, y coordinates parallel and perpendicular, respectively, to the wall wetted by the flow ($x = y = 0$: stagnation point and leading edge of the plate, respectively)

δ^* displacement thickness of the boundary layer
$$\int_{y=0}^{\infty} (1 - u/U) dy$$

δ momentum thickness of the boundary layer
$$\int_{y=0}^{\infty} u/U(1 - u/U) dy$$

δ_1 measure of the boundary layer thickness

l plate length or wing chord, respectively

b plate width

(b) Velocities

u, v velocity components in the friction layer, parallel and perpendicular to the wall

$U(x)$ potential velocity outside of the friction layer

U_0 free stream velocity

$v_0(x)$ given suction velocity at the wall $v_0 < 0$: suction

(c) Other Quantities

τ_o	wall shearing stress
$\tau_{o\infty}$	wall shearing stress for asymptotic solution of boundary layer on plate in longitudinal flow with homogeneous suction
Q	total suction quantity $\left(b \int_{x=0}^l v_o dx \right)$
c_Q	dimensionless mass coefficient of suction; $c_Q > 0$: suction $\left(\frac{-Q}{lbU_o} \right)$
c^*_Q	reduced mass coefficient of suction $\left(c_Q \sqrt{\frac{U_o l}{v}} \right)$
η	dimensionless distance from wall (y/δ_l)
$F_1(\eta)$, $F_2(\eta)$	basic functions for velocity distribution in boundary layer, equations (8), (9)
K	form parameter of boundary layer profiles, equation (6)
λ, λ_l	dimensionless boundary layer thickness, equations (12), (13)
κ, κ_l	dimensionless momentum thickness, equations (22), (23)
ξ	dimensionless length of boundary layer $\left(\frac{-v_o}{U_o} \right)^2 \frac{U_o x}{v}$

III. THE EQUATIONS OF THE BOUNDARY LAYER

WITH SUCTION

Following we shall consider the plane problem, thus the boundary layer on a cylindrical body in a flow (fig. 1). x, y are assumed to be the coordinates along the wall and perpendicular to the wall, respectively, U_o the free stream velocity, $U(x)$ the potential flow outside of the friction layer, and $u(x, y)$, $v(x, y)$ the velocity distribution in the friction layer. Suction and blowing is introduced into the calculation by having along the wall a normal velocity $v_o(x)$ prescribed which is different from zero and generally variable with x :

$$v_o(x) > 0: \text{blowing}; \quad v_o(x) < 0: \text{suction}$$

v_o/U_o may be assumed to be very small (0.01 to 0.0001). Only the case of continuous suction will be considered, where, therefore, $v_o(x)$ is a continuous function of x . One may visualize this case as realized by a porous wall. The tangential velocity at the wall should, for every case, equal zero. The boundary layer differential equations with boundary conditions are for the steady flow case

$$u \frac{\partial u}{\partial x} + v \frac{\partial u}{\partial y} = U \frac{du}{dx} + v \frac{\partial^2 u}{\partial y^2} \quad (1)$$

$$\frac{\partial u}{\partial x} + \frac{\partial v}{\partial y} = 0 \quad (1a)$$

$$\left. \begin{array}{l} y = 0: \quad u = 0; \quad v = v_0(x) \\ y = \infty: \quad u = U(x) \end{array} \right\} \quad (2)$$

The system of equations (1), (2) differs from the ordinary boundary layer theory merely by the fact that one of the boundary conditions for $y = 0$ is changed from $v = 0$ to $v = v_0(x) \neq 0$. Thereby the character of the solutions changes decisively: the solutions differ greatly according to whether it is a case of $v_0 > 0$ (blowing) or $v_0 < 0$ (suction).

A special solution of the equations (1), (2) which forms the basis for the theory of the boundary layer with suction and is used again below is the solution for the plane plate in longitudinal flow with homogeneous suction, thus $v_0(x) = v_0 = \text{const} < 0$ and $U(x) = U_0$. For this case the boundary layer thickness becomes constant at some distance from the leading edge of the plate; also, the velocity distribution becomes independent of x (reference 5). From $\frac{\partial u}{\partial x} = 0$ follows because of the continuity $\frac{\partial v}{\partial y} = 0$ and hence

$$v(x, y) = v_0 = \text{Constant}$$

From equation (1) then follows for the velocity distribution

$$u(x, y) = u(y) = U_0 \left(1 - e^{-\frac{yv_0}{v}} \right) = U_0 \left(1 + e^{-\frac{y}{\delta^*_{\infty}}} \right) \quad (3)$$

with

$$\delta^*_{\infty} = \frac{v}{-v_0} \quad (4)$$

signifying the displacement thickness of the asymptotic solution. The wall shearing stress for this solution is:

$$\tau_{0\infty} = \mu \left(\frac{\partial u}{\partial y} \right)_0 = -\rho U_0 v_0 \quad (4a)$$

It is independent of the viscosity. This asymptotic solution is one of the very rare cases where the boundary layer differential equations can be integrated in closed form.

For solution of the boundary layer differential equations (1), (2) for the general case where the contour of the body and hence $U(x)$ and also $v_0(x)$ are prescribed arbitrarily one could consider developing the velocity distribution from the stagnation point into a series in terms of x in the same way as for impermeable wall (reference 11); the coefficients of this series then are functions dependent on y for which ordinary differential equations result. K. Bussmann (reference 17) applied this method for the circular cylinder; with a very considerable expenditure of time for calculations the aim was attained there. However, for slenderer body shapes the difficulties of convergence increase so much that this method which works directly with the differential equations is useless for practical purposes.

I V. THE GENERAL APPROXIMATION METHOD FOR
 ARBITRARY PRESSURE DISTRIBUTION
 AND ARBITRARY DISTRIBUTION OF
 THE SUCTION VELOCITY

(a) The Expression for the Velocity Distribution

For that reason one applies an approximation method which uses instead of the differential equations the momentum theorem which represents an integral of these differential equations. By integration of the equations (1), (2) over y between the limits $y = 0$ and $y = \infty$ one obtains in the known manner (reference 18):

$$U^2 \frac{d\vartheta}{dx} + (2\vartheta + \delta^*) U \frac{dU}{dx} - U v_0 = \frac{\tau_0}{\rho} \quad (5)$$

δ signifies the momentum thickness, δ^* the displacement thickness, and

$\tau_0 = \mu \left(\frac{\partial u}{\partial y} \right)_0$ the wall shearing stress. The approximation method for

calculation of the boundary layer to be chosen here proceeds in such a manner that a plausible expression is given for the velocity distribution in the boundary layer $u(x, y)$ which is contained in equation (5) in δ , δ^* and τ_0 . Thus an ordinary differential equation for $\delta(x)$ results from equation (5); after this differential equation has been solved one obtains the remaining characteristics of the boundary layer $\delta^*(x)$, $\tau_0(x)$, and the velocity distribution $u(x, y)$ in the boundary layer. The usefulness of this approximation method depends to a great extent on whether one succeeds in finding for $u(x, y)$ an expression by appropriate functions.

Pohlhausen (reference 15) first carried out this method for the boundary layer with impermeable wall. The velocity profiles in the boundary layer were approximated by a one-parametric family and the approximation function for the velocity distribution expressed as a polynome of the fourth degree. The coefficients of this polynome are determined by fulfilling for the velocity profiles a few boundary conditions which result from the differential equations of the boundary layer. This method proved to be satisfactory for the boundary layer without suction.

Thus one proceeds in the same way for the boundary layer with suction. For the velocity distribution in the boundary layer one chooses the one-parametric expression

$$\frac{u}{U} = F_1(\eta) + K F_2(\eta); \quad \eta = \frac{y}{\delta_1(x)} \quad (6)$$

$F_1(\eta)$ and $F_2(\eta)$ are fixed prescribed functions which are immediately expressed explicitly; $K = K(x)$ is a form parameter of the boundary layer profiles, the distribution of which along the length is dependent on the body shape and the suction law; $\delta_1(x)$ is a measure for the local boundary layer thickness. The connection between δ_1 and δ^* and δ is given later. It proved useful to choose other expressions for the functions $F_1(\eta)$ and $F_2(\eta)$ than Pohlhausen for the impermeable wall. For the velocity profile according to equation (6) the following five boundary conditions are prescribed; they all follow from the differential equations of the boundary layer with suction, equation (1), (2):

$$y = 0: \quad u = 0; \quad v \frac{\partial u}{\partial y} = U \frac{\partial U}{\partial x} + v \frac{\partial^2 u}{\partial y^2} \quad (7a, b)$$

$$y = \infty: \quad u = U_0; \quad \frac{\partial u}{\partial y} = 0; \quad \frac{\partial^2 u}{\partial y^2} = 0 \quad (7c, d, e)$$

The selection of $F_1(\eta)$ and $F_2(\eta)$ is to be made from the view point that a few typical special cases of velocity profiles of the boundary layer with suction are represented by equation (6) as satisfactorily as possible. In particular we shall require the asymptotic suction profile according to equation (3) to be contained in the expression (6). This condition is satisfied if one puts

$$F_1(\eta) = 1 - e^{-\eta} \quad (8)$$

and correlates the values $K = 0$ and $\delta_1 = \delta^*$ to the asymptotic suction profile. Furthermore, the expression (6) naturally should yield usable results also for the limiting case of disappearing suction. To this purpose a good presentation of a typical boundary layer profile without suction is required. One chooses as this profile the plate flow for impermeable wall according to Blasius (reference 11). Since no convenient analytical formula exists for the exact solution of this case, a good approximation formula for Blasius' plate profile is needed. It is found that the function $\frac{u}{U_\infty} = \sin(a\eta)$ gives a very good approximation to the Blasius profile ($a = \text{Constant}$)¹. Thus one puts

$$0 < \eta \leq 3: \quad F_2(\eta) = F_1 - \sin\left(\frac{\pi}{6}\eta\right) \quad (9)$$

$$\eta \geq 3: \quad F_2(\eta) = F_1 - 1 = -e^{-\eta}$$

and then obtains with $K = -1$ a good approximation for the plate flow without suction. The corresponding value of δ_1 is given later. The functions $F_1(\eta)$ and $F_2(\eta)$ are given in figure 2 and table 1. Thus one has for the velocity distribution in the boundary layer the expression:

¹That the sine function is a good approximation for the velocity distribution at the plane plate without suction, resulted from an investigation of Mr. Iglisch about the asymptotic behavior of the plane stagnation point flow for large blowing quantity (reference 20).

$$0 \leq \eta \leq 3: \frac{u}{U} = 1 - e^{-\eta} + K \left[1 - e^{-\eta} - \sin\left(\frac{\pi}{6}\eta\right) \right] \quad (10)$$

$$\eta \geq 3: \frac{u}{U} = 1 - (K + 1)e^{-\eta}$$

By selection of the functions F_1 and F_2 the boundary conditions (7a,c,d,e) are per se satisfied. The last boundary condition, equation (7b), results, because of

$$\frac{\tau_0}{\rho} = \nu \left(\frac{\partial u}{\partial y} \right)_0 = \frac{\nu U}{\delta_1} \left[1 + K \left(1 - \frac{\pi}{6} \right) \right] \quad (11)$$

in the following qualifying equation for K :

$$\frac{\nu_0 U}{\delta_1} \left[1 + K \left(1 - \frac{\pi}{6} \right) \right] = UU' - \nu \frac{U}{\delta_1^2} (1 + K)$$

and from it with

$$\lambda = \frac{\delta_1^2 U'}{\nu} \quad (12)$$

$$\lambda_1 = \frac{-\nu_0 \delta_1}{\nu} \quad (13)$$

for K the equation

$$K = \frac{\lambda + \lambda_1 - 1}{1 - \lambda_1 \left(1 - \frac{\pi}{6} \right)} \quad (14)$$

λ and λ_1 are two dimensionless boundary layer parameters. A quantity analogous to λ was already used by Pohlhausen for the boundary layer without suction; λ_1 is newly added by the suction. For the asymptotic suction profile with $\delta_1 = \delta$, $\lambda_1 = 1$ according to equation (4). The form parameter K as a function of λ and λ_1 is represented in figure 3.

(b) The Differential Equation for the Momentum Thickness

In order to obtain by means of the expressions (6), (8), and (9) from equation (5) the differential equation for the momentum thickness one must first set up the relations between δ , δ^* , and δ_1 . For the displacement thickness there results:

$$\frac{\delta^*}{\delta_1} = \int_{\eta=0}^{\infty} (1 - F_1) d\eta - K \int_0^{\infty} F_2 d\eta \quad (15)$$

The calculation of the integrals gives:

$$\frac{\delta^*}{\delta_1} = 1 - K \left(2 - \frac{6}{\pi} \right) = g^*(K) \quad (16)$$

For the momentum thickness one obtains:

$$\frac{\delta}{\delta_1} = \int_0^{\infty} (F_1 + KF_2)(1 - F_1 - KF_2) d\eta$$

$$\frac{\delta}{\delta_1} = C_0 + C_1 K + C_2 K^2 = g(K) \quad (17)$$

The calculation of the integrals gives:

$$C_0 = \int_0^{\infty} F_1(1 - F_1) d\eta = \frac{1}{2} \quad (18a)$$

$$C_1 = \int_0^{\infty} (F_2 - F_1 F_2) d\eta = -1 + \frac{6}{\pi} - \frac{\pi}{3} \frac{1 + \frac{\pi}{6e^3}}{1 + \left(\frac{\pi}{6}\right)^2} = 0.06656 \quad (18b)$$

$$C_2 = - \int_0^\infty F_2^2 d\eta = -3 + \frac{12}{\pi} - \frac{\pi}{3} \frac{1 + \frac{\pi}{6e^3}}{1 + \left(\frac{\pi}{6}\right)^2} = -0.02358 \quad (18c)$$

Hence

$$C_1 - C_2 = 2 - \frac{6}{\pi} = 0.09014$$

Thus there is

$$\frac{\delta}{\delta_1} = \frac{1}{2} + 0.06656K - 0.02358K^2 = g(K) \quad (17a)$$

For the form parameter of the boundary layer profiles δ^*/δ used later one obtains therefore

$$\frac{\delta^*}{\delta} = \frac{1 - K\left(2 - \frac{6}{\pi}\right)}{\frac{1}{2} + C_1K + C_2K^2} = \frac{1 - 0.09014K}{\frac{1}{2} + 0.06656K - 0.02358K^2} \quad (19)$$

Furthermore there results according to equations (11) and (17):

$$\frac{\tau_0 \delta}{\mu} = g \left[1 + K \left(1 - \frac{\pi}{6} \right) \right] = f(K) \quad (20)$$

The functions $g(K)$, δ^*/δ and $\tau_0 \delta_1 / \mu U$ according to equation (11) are represented in figure 4 and table 2.

In order to derive from equation (5) a differential equation for $\delta(x)$ one writes equation (5) in the form

$$\frac{U \delta}{V} \frac{d\delta}{dx} + \left(2 + \frac{\delta^*}{\delta} \right) \frac{U' \delta^2}{V} = \frac{\tau_0 \delta}{\mu} \frac{\delta}{U} \quad (21)$$

Furthermore one introduces according to Holstein and Bohlen (reference 19)

$$\frac{U'g^2}{v} = \kappa = \lambda g^2 \quad (22)$$

and

$$\frac{-v_0 \vartheta}{v} = \kappa_1 = \lambda_1 g \quad (23)$$

With

$$Z = \frac{g^2}{v} \quad (24)$$

then

$$\kappa = ZU'; \quad \kappa_1 = -v_0 \sqrt{\frac{Z}{v}} \quad (25)$$

is valid. With equations (22) to (25) as well as equation (20) the differential equation (21) is transformed into

$$\frac{1}{2} U \frac{dZ}{dx} + \left[2 + \frac{1 - K(2 - \frac{6}{\pi})}{g(K)} \right] \kappa + \kappa_1 = f(K) \quad (26)$$

If one finally puts for abbreviation:

$$G(\kappa, \kappa_1) = 2f - 2\kappa \left[2 + \frac{1 - K(2 - \frac{6}{\pi})}{g(K)} \right] - 2\kappa_1 \quad (27)$$

the differential equation for $Z(x)$ becomes:

$$\frac{dZ}{dx} = \frac{G(\kappa, \kappa_1)}{U}; \quad \kappa = ZU'; \quad \kappa_1 = -v_0 \sqrt{\frac{Z}{v}}$$

(28)

If the function $G(\kappa, \kappa_1)$ is known, the integral curve $Z(x)$ can be calculated from this equation by means of the isocline method.

For carrying out the calculation in practice it is useful to introduce dimensionless quantities. One forms them with the aid of the free stream velocity U_0 and a length of reference l (for instance, chord of the wing). Thus one puts

$$Z^* = \frac{ZU_0}{l}; \quad x^* = \frac{x}{l}; \quad \frac{-v_0(x^*)}{U_0} \sqrt{\frac{U_0 l}{v}} = f_1(x^*) \quad (29)$$

Then equation (28) becomes:

$$\frac{dZ^*}{dx^*} = \frac{G(\kappa, \kappa_1)}{U_0/U_0}; \quad \kappa = Z^* \frac{l}{U_0} \frac{dU}{dx}; \quad \kappa_1 = f_1(x^*) \sqrt{Z^*} \quad (30)$$

The function $G(\kappa, \kappa_1)$ is calculated as follows: First, one obtains κ and κ_1 as functions of λ and λ_1 from equations (22) and (23), if one takes the connection between K and λ, λ_1 according to equation (14) into consideration:

$$\left. \begin{aligned} \kappa &= g^2(K)\lambda = g^2(\lambda, \lambda_1)\lambda \\ \kappa_1 &= g(K)\lambda_1 = g(\lambda, \lambda_1)\lambda_1 \end{aligned} \right\} \quad (31)$$

From equations (27) and (31) follows:

$$\begin{aligned} \frac{1}{2}G &= g \left[1 + K \left(1 - \frac{\pi}{6} \right) \right] - \lambda g^2 \left[2 + \frac{1 - K \left(2 - \frac{\pi}{6} \right)}{g} \right] - \lambda_1 g \\ \frac{1}{2}G &= g \left\{ 1 + K \left(1 - \frac{\pi}{6} \right) - 2\lambda g - \lambda \left[1 - K \left(2 - \frac{\pi}{6} \right) \right] - \lambda_1 \right\} \\ G &= 2gF(\lambda, \lambda_1) \end{aligned} \quad (32)$$

with

$$F(\lambda, \lambda_1) = 1 + K\left(1 - \frac{\pi}{6}\right) - 2\lambda g - \lambda \left[1 - K\left(2 - \frac{6}{\pi}\right)\right] - \lambda_1 \quad (33)$$

Hence G can be calculated first as function of λ, λ_1 and then, because of equation (31), also as function of κ, κ_1 .

The functions $\kappa(\lambda, \lambda_1)$ and $\kappa_1(\lambda, \lambda_1)$ are represented in figure 5 and table 3. The function thus determined $G(\kappa, \kappa_1)$ is given in figure 6 and table 3.

(c) Stagnation Point and Separation Point

The behavior of the differential equation (28) at the stagnation point where $U = 0$ requires special considerations. In order that the initial inclination of the integral curve $(dZ/dx)_0$ at this point be of finite value, $G(\kappa, \kappa_1)$ must equal zero. This gives the corresponding initial values κ_0, κ_{10} . Since the function $g(K)$ does not have a zero for the values of K considered (compare fig. 4) the determination of the initial values κ_0, κ_{10} amounts to the zeros of

$$F(\lambda_0, \lambda_{10}) = 0 \quad (34)$$

The resulting initial values at the stagnation point λ_0, λ_{10} are given in table 4, together with the initial values κ_0, κ_{10} calculated additionally according to equation (31). To each pair of values κ_0, κ_{10} corresponds a mass coefficient of suction which results from

$$\frac{\vartheta_0^2}{\nu} U_0' = \kappa_0; \quad \frac{-v_0(0)\vartheta_0}{\nu} = \kappa_{10}$$

as

$$\frac{-v_0(0)}{\sqrt{U_0' \nu}} = \frac{\kappa_{10}}{\sqrt{\kappa_0}} = C_0$$

In figure 7 the initial values κ_0 and κ_{10} are plotted against the local mass coefficient at the stagnation point. The initial value Z_0 corresponding to κ_0 is obtained by

$$Z_0 = \frac{\kappa_0}{U_0'} \quad (35)$$

The following connection exists between the distribution function of the suction $f_1(x) = \frac{-v_0(x)}{U_0} \sqrt{\frac{U_0 l}{\nu}}$ and C_0 : $U_0' = K_1 U_0 / l$, K_1 being a profile constant. Thus there is

$$\sqrt{U_0' \nu} = U_0 \sqrt{K_1} \sqrt{\frac{\nu}{U_0 l}}$$

and

$$C_0 = \frac{-v_0(0)}{\sqrt{U_0' \nu}} = \frac{-v_0(0)}{U_0} \sqrt{\frac{U_0 l}{\nu}} \frac{1}{\sqrt{K_1}}$$

$$C_0 = \frac{f_1(0)}{\sqrt{K_1}} \quad (36)$$

The determination of the initial values of the integral curve proceeds, therefore, as follows: With the given initial value of the suction velocity at the stagnation point $f_1(0)$ one first determines C_0 according to equation (36). One obtains the corresponding initial values κ_0 and κ_{10} from figure 7, and according to equation (35) the initial value Z_0 of the integral curve. If the suction does not begin at the stagnation point but further downstream, $C_0 = 0$; $\kappa_{10} = 0$ and according to figure 7

$$\kappa_0 = 0.0709; \quad Z_0 = \frac{0.0709}{U_0'}$$

Separation point. - The separation point is defined by the fact that the wall shearing stress there equals zero. This gives for K , according to equation (11), the value $K = \frac{-6}{6 - \pi} = -2.099$. For the asymptotic suction profile $K = 0$; this is simultaneously the greatest possible value of K . To $K = -2.099$ corresponds the value $\lambda = \frac{-\pi}{6 - \pi} = -1.099$ for all λ_1 , and

$\kappa = -0.0721$ for all κ_1 . However, if one would want to carry the boundary layer calculation up to this point, certain difficulties result in the last part shortly ahead of this point, since the correlation between κ and λ is not unequivocal there (compare fig. 4). The function $G(\kappa, \kappa_1)$ against κ also is not unequivocal shortly ahead of this point. Thus it is useful to select a point situated somewhat further upstream as separation point where the boundary layer calculation has to stop. Such a point results if one chooses the κ -value of an exact separation profile according to Hartree (reference 13). For this latter there is:

$$\text{separation: } \kappa_A = \left(\frac{\delta^2}{V} \frac{dU}{dx} \right)_A = -0.0682 \quad (37)$$

One defines this point as separation point of the present boundary layer calculation for all mass coefficients of suction. The following table gives a survey of the values of δ and δ^* at the separation point for four different calculation methods:

Case	$\frac{\delta^2}{V} U' = \kappa_A$	$\frac{\delta^2}{V} U' = \lambda_A^*$	$\frac{\delta^*}{\delta}$
New method: (sine approximation)	(-0.0721)	(-1.55)	(4.64)
Pohlhausen P4 (reference 15)	-0.1567	-1.92	3.50
Exact Hartree (reference 13)	-0.0682	-1.22	4.03
Exact Howarth (reference 14)	-0.0841	-1.25	3.84

The selection of the separation point thus made is somewhat arbitrary; however, it may be accepted unhesitatingly since, as is well known, the approximation methods for the boundary layer calculation in the region of the pressure rise are always somewhat uncertain and only a rough estimate but no exact calculation of the boundary layer parameters is possible here. For the same reason one may also accept the fact that for the present case the velocity distribution u/U_0 partly assumes, shortly ahead of the separation point, values which are slightly larger than 1.

(d) Performance of the Calculation for the General Case

By means of the system of formulas given above one may perform the calculation of the boundary layer for an arbitrarily prescribed body shape and an arbitrary distribution of the suction velocity along the wall in the flow. It takes the following course:

To the distribution of the suction velocity $-v_o(x)$ corresponds the total suction quantity

$$Q = \int_{x=0}^l v_o(x) dx = -c_Q U_o b l$$

and the reduced mass coefficient

$$c_Q^* = c_Q \sqrt{\frac{U_o l}{v}} \quad (38)$$

and the reduced suction distribution function according to equation (29):

$$f_l(x^*) = \frac{-v_o(x^*)}{U_o} \sqrt{\frac{U_o l}{v}}$$

Thus there is

$$c_Q^* = \int_{x^*=0}^l f_l(x^*) dx^* \quad (39)$$

If the suction begins at the stagnation point, one determines with $K_1 = \frac{l}{U_o} \left(\frac{dU}{dx} \right)_o$ the mass coefficient c_o at the stagnation point according to equation (36). Then one obtains κ_o and κ_{lo} from figure 7 and Z_o according to equation (35). With these initial values the differential equation (30) can now be graphically integrated by means of the diagram in figure 6. The calculation is carried out up to the point where κ reaches the value $\kappa_A = -0.0682$. This integration immediately yields Z^* , κ , κ_1 as function of x^* , with

$$\sqrt{Z^*} = \frac{\delta}{l} \sqrt{\frac{U_0 l}{v}} \quad (40)$$

The remaining boundary layer parameters then result as follows: By means of figure 5 one obtains after κ and κ_1 the parameters λ and λ_1 and additionally from figure 3 the form parameter K . After K one obtains from figure 4 the form parameter δ^*/δ and thus

$$\frac{\delta^*}{l} \sqrt{\frac{U_0 l}{v}} = \frac{\delta^*}{\delta} \sqrt{Z^*}$$

From equation (20) one then also obtains the wall shearing stress τ_0

$$\frac{\tau_0}{\mu U} \sqrt{\frac{v l}{U_0}} = \frac{f(K)}{\sqrt{Z^*}} \quad (40a)$$

Finally, the parameter δ_1 is required for the velocity distribution in the boundary layer. According to equations (6), (7), and (40):

$$\eta = \frac{y}{\delta_1} = \frac{y}{\delta} g(K) = \frac{y}{l} \sqrt{\frac{U_0 l}{v}} \frac{g(K)}{\sqrt{Z^*}} \quad (41)$$

Examples of such boundary layer calculations are given in chapter VI.

V. SPECIAL CASES

A. WITHOUT SUCTION

Our general system of formulas is to be specialized in this section for a few typical special cases for which one can partly give solutions in closed form. First, the case without suction in particular shall be treated for which, naturally, our equations also must give satisfactory results. This case one obtains for $v_0(x) = 0$; then

$$\lambda_1 \equiv 0; \quad \kappa_1 \equiv 0 \quad (\text{without suction})$$

and equation (14) is transformed into

$$K = \lambda - 1 \quad (42)$$

Therewith, according to equation (17):

$$\begin{aligned} \frac{\partial}{\partial \lambda} = g(\lambda) &= \frac{1}{2} + c_1(\lambda - 1) + c_2(\lambda - 1)^2 \\ &= \frac{1}{2} + 0.06656(\lambda - 1) - 0.02358(\lambda - 1)^2 \end{aligned} \quad (43)$$

The differential equation (28) for the momentum thickness becomes

$$\frac{dZ}{dx} = \frac{G(\kappa)}{U}; \quad \kappa = ZU' \quad (44)$$

$G(\kappa)$ is, according to equation (32) and (33):

$$G = 2gF(\lambda) \quad (45)$$

$$\begin{aligned} F(\lambda) &= 1 + (\lambda - 1)\left(1 - \frac{\pi}{6}\right) - 2\lambda \left[\frac{1}{2} + c_1(\lambda - 1) + c_2(\lambda - 1)^2\right] \\ &\quad - \lambda \left[1 + (1 - \lambda)\left(2 - \frac{6}{\pi}\right)\right] \\ F(\lambda) &= -2c_2\lambda^3 + \left(2c_2 - 2 + \frac{6}{\pi}\right)\lambda^2 + \left(1 - \frac{6}{\pi} - \frac{\pi}{6}\right)\lambda + \frac{\pi}{6} \end{aligned} \quad (46)$$

Furthermore, according to equation (31):

$$\kappa = g^2\lambda = \lambda \left[\frac{1}{2} + c_1(\lambda - 1) + c_2(\lambda - 1)^2\right]^2 \quad (47)$$

The values of G and κ calculated according to equations (43), (45), (46), (47) are given in table 3.

(a) The Plane Plate in Longitudinal Flow

The boundary layer at the plate in longitudinal flow without suction (Blasius) with $U = U_0$ is obtained for $\lambda = \kappa = 0$. Then, according to equations (42) to (46):

$$\left. \begin{aligned} K &= -1 \\ g(0, 0) &= \frac{1}{2} - c_1 + c_2 = \frac{6}{\pi} - \frac{3}{2} \\ F(0, 0) &= \frac{\pi}{6} \\ G(0, 0) &= 2\frac{\pi}{6}\left(\frac{6}{\pi} - \frac{3}{2}\right) = 2 - \frac{\pi}{2} = 0.429 \end{aligned} \right\} \quad (48)$$

With the initial value $Z_0 = 0$ the integration of equation (44) then

gives: $Z = \left(2 - \frac{\pi}{2}\right) \frac{x}{U_0}$ or

$$\vartheta = \sqrt{\frac{4 - \pi}{2}} \sqrt{\frac{vx}{U_0}} = 0.655 \sqrt{\frac{vx}{U_0}} \quad (49)$$

For the form parameter δ^*/ϑ follows from equation (19):

$$\frac{\delta^*}{\vartheta} = 2 \frac{\pi - 2}{4 - \pi} = 2.66 \quad (50)$$

and thus for the displacement thickness

$$\delta^* = (\pi - 2) \sqrt{\frac{2}{4 - \pi}} \sqrt{\frac{v_x}{U_o}} = 1.740 \sqrt{\frac{v_x}{U_o}} \quad (51)$$

For the coefficient of the total friction drag $c_f = \frac{W_R}{\frac{1}{2} U_o^2 b l}$ of the plate of the width b and the length l , wetted on one side, one obtains because of $c_f = \frac{2^3 l}{l}$

$$c_f = \sqrt{8 - 2\pi} \sqrt{\frac{v}{U_o l}} = 1.308 \sqrt{\frac{v}{U_o l}} \quad (52)$$

Finally, the velocity distribution is, according to equation (10),

$$0 \leq \eta \leq 3: \quad u = U_o \sin\left(\frac{\pi}{6}\eta\right) \quad (53)$$

$$\eta \geq 3: \quad u = U_o$$

Therein is $\eta = \frac{y}{\delta_1}$ and

$$\delta_1 = \frac{\pi}{3} \sqrt{\frac{2}{4 - \pi}} \sqrt{\frac{v_x}{U_o}} = 1.60 \sqrt{\frac{v_x}{U_o}} \quad (54)$$

In figure 8 the velocity distribution according to equations (53) and (54) is compared with the exact solution of Blasius; the agreement is very good. Furthermore the characteristics of the boundary layer according to the present approximation calculation are compared with the values of the exact solution of Blasius in the following table. For further comparison the values according to the approximation method of Pohlhausen (reference 15) also have been given. The agreement of our new approximation method with the exact solution is excellent for all boundary layer parameters; the drag coefficient, in particular, shows an error of only 2 percent.

Coefficients of the Boundary Layer at the Flat Plate
in Longitudinal Flow Without Suction

Calculation method	$\delta^* \sqrt{\frac{U_o}{v x}}$	$\delta \sqrt{\frac{U_o}{v x}}$	$\frac{\delta^*}{\delta}$	$c_f \left(\frac{U_o l}{v} \right)^{\frac{1}{2}}$	$\frac{\tau_o}{\mu} \frac{\delta}{U_o}$
New method (sine approximation)	1.740	0.655	2.66	1.310	0.215
Pohlhausen P4 (reference 15)	1.750	0.685	2.55	1.370	0.234
Exact (Blasius)	1.721	0.664	2.59	1.328	0.220

The deviations of our sine approximation from the exact solution are, for most characteristics, even somewhat smaller than in the Pohlhausen method.

(b) The Plane Stagnation Point Flow

For the plane stagnation point flow the velocity of the potential flow $U(x) = u_1 x$. All boundary layer characteristics are in this case independent of the length x . The initial value of the momentum thickness Z_o is obtained from equation (44) for $G(\kappa_o) = 0$. Since $g(K)$ does not vanish in the range of the values of K considered, there must be $F(\lambda_o) = 0$. From equation (46) one finds as zero of $F(\lambda)$ the value

$$\lambda_o = 0.3547 \quad (\text{stagnation point without suction}) \quad (54)$$

The corresponding values of K and κ according to equations (42) and (47) are $K_o = -0.6453$ and $\kappa_o = 0.0709$; furthermore there is, according to equation (43): $g(\lambda_o) = 0.447$. Therewith the momentum thickness for the plane stagnation point flow becomes:

$$\delta = \sqrt{\kappa_o} \sqrt{\frac{v}{u_1}} = 0.266 \sqrt{\frac{v}{u_1}} \quad (55)$$

The form parameter δ^*/δ results from equation (19) as $\delta^*/\delta = 2.37$; therewith one has

$$\delta^* = 2.37 \sqrt{k_o} \sqrt{\frac{v}{u_1}} = 0.630 \sqrt{\frac{v}{u_1}} \quad (56)$$

Furthermore, according to equation (43): $\delta_1 = 0.595 \sqrt{\frac{v}{u_1}}$. Thus there results from equation (11) for the wall shearing stress:

$$\frac{\tau_o}{\mu U} \sqrt{\frac{v}{u_1}} = 1.163 \quad (57)$$

The velocity distribution results from equation (10) as:

$$\left. \begin{array}{l} 0 \leq \eta \leq 3: \frac{u}{U_o} = 0.3574(1 - e^{-\eta}) + 0.6453 \sin\left(\frac{\pi}{6}\eta\right) \\ \eta \geq 3: \frac{u}{U_o} = 1 - 0.3574e^{-\eta} \end{array} \right\} \quad (58)$$

with

$$\eta = \frac{y}{\delta_1} = 1.68y \sqrt{\frac{u_1}{v}} \quad (58a)$$

Figure 8 gives a comparison between velocity distribution according to equation (58) and the exact solution by Hiemenz (reference 12); here also the agreement is satisfactory. Furthermore the characteristics of the boundary layer according to the present calculation are again compared with the exact solution by Hiemenz and with the approximate calculation by Pohlhausen in the following table.

Coefficients of the Boundary Layer of the Plane

Stagnation Point Flow without Suction

Calculation method	$\delta \sqrt{\frac{u_1}{v}}$	$\delta^* \sqrt{\frac{u_1}{v}}$	$\frac{\delta^*}{\delta}$	$\frac{\tau_0}{\mu U} \sqrt{\frac{v}{u_1}}$	$\frac{\tau_0 \delta}{\mu U}$
New method (sine approximation)	0.266	0.630	2.37	1.163	0.310
Pohlhausen P4 (reference 15)	0.278	0.641	2.31	1.19	0.331
Exact (Hiemenz)	0.292	0.648	2.21	1.234	0.360

The agreement of the new method with the exact solution is for this case somewhat less satisfactory than for the plane plate; neither is it quite as good as the approximation of Pohlhausen. But even here the new method yields still very useful values.

B. WITH SUCTION

In this section a few cases with suction will be treated for which the solutions can be given in closed form. First we shall treat the boundary layer at the plate in longitudinal flow with homogeneous suction, already investigated formerly (reference 6). The following results are considerably more accurate than those former ones.

(a) Growth of the Boundary Layer for the Plate

in Longitudinal Flow with Homogeneous Suction

For this case the boundary layer is at large distance from the leading edge of the plate independent of x ; hence all boundary layer parameters are constant. The corresponding asymptotic solution has been given already in equations (3), (4), (4a). The applying values are:

$$\left. \begin{aligned} \delta^*_{\infty} &= \frac{v}{-v_0}; & \frac{\delta^*}{\delta} &= 2; & \tau_{0\infty} &= -\rho U_0 v_0; & K &= 0 \\ \delta_1 &= \delta^*_{\infty}; & \lambda_1 &= 1; & \kappa_1 &= \frac{1}{2} \end{aligned} \right\} \quad (59)$$

One now calculates the growth of the boundary layer from the value zero at the leading edge of the plate to the given asymptotic value. In our system of formulas one has to put for it:

$$\lambda \equiv 0; \quad \kappa \equiv 0$$

Therewith becomes according to equation (14) with the abbreviation

$$1 - \frac{\pi}{6} = c = 0.4764 \quad (60)$$

$$K = \frac{\lambda_1 - 1}{1 - c\lambda_1} \quad (61)$$

and according to equation (17)

$$\frac{\delta}{\delta_1} = g(0, \lambda_1) = \frac{p_0 + p_1\lambda_1 + p_2\lambda_1^2}{(1 - c\lambda_1)^2} \quad (62)$$

with

$$p_0 = -\frac{3}{2} + \frac{6}{\pi} = 0.40986$$

$$p_1 = 3 + \frac{\pi}{6} - \frac{12}{\pi} - \frac{\pi}{6}c_1 = 0.06656 \quad (62a)$$

$$p_2 = -2 + \frac{6}{\pi} + \frac{1}{2} \left(1 - \frac{\pi}{6}\right)^2 + \frac{\pi}{6}c_1 = 0.05819$$

Furthermore there is according to equation (16)

$$\frac{\delta^*}{\delta_1} = 3 - \frac{6}{\pi} + \lambda_1 \left(-3 + \frac{6}{\pi} + \frac{\pi}{6}\right) \quad (63)$$

The wall shearing stress becomes according to equations (11) and (13):

$$\tau_0 = \mu \frac{U_0}{\delta_1} \frac{\frac{\pi}{6}}{1 - c\lambda_1} = -\rho v_0 U_0 \frac{\frac{\pi}{6}}{\lambda_1(1 - c\lambda_1)} \quad (64)$$

The differential equation (28) assumes for the present case the form:

$$\frac{dZ}{dx} = \frac{G(0, \kappa_1)}{U_0}; \quad \kappa_1 = -v_0 \sqrt{\frac{Z}{v}}; \quad v_0 = \text{Constant} < 0 \quad (65)$$

The integration of this differential equation requires the explicit expression for $G(0, \kappa_1)$. According to (32) and (33):

$$G(0, \kappa_1) = 2g \left(\frac{\frac{\pi}{6}}{1 - c\lambda_1} - \lambda_1 \right) = 2g(1 - \lambda_1) \frac{\frac{\pi}{6} - c\lambda_1}{1 - c\lambda_1} \quad (66)$$

Thus $G(0, \kappa_1) = 0$ for $\lambda_1 = 1$. Therefore $\lambda_1 = 1$ is a solution of the momentum equation; it corresponds to the asymptotic solution. The initial value at the leading edge of the plate is $\lambda_1 = 0$. For the length of growing boundary layer λ_1 varies from 0 to 1.

If one introduces as dimensionless distance along the plate

$$\xi = \frac{U_0 x}{v} \left(\frac{v_0}{U_0} \right)^2 \quad (67)$$

the differential equation (65) can be written in the form:

$$\frac{d(\kappa_1^2)}{d\xi} = G(\kappa_1) \quad (68)$$

$$\text{Initial value: } \xi = 0; \quad \kappa_1 = 0 \quad (68a)$$

The connection between κ_1 and λ_1 is given by

$$\kappa_1 = \lambda_1 g(\lambda_1) \quad (69)$$

with $g(\lambda_1)$ according to equation (62).

The differential equation (68) can be solved according to the isocline method. For the present case, however, an analytical solution, too, is possible which is preferable. From equation (69) first follows:

$$2\kappa_1 \frac{d\kappa_1}{d\lambda_1} \frac{d\lambda_1}{d\xi} = G(\kappa_1) \quad (70)$$

Here all quantities can be best expressed by λ_1 so that a differential equation for $\lambda_1(\xi)$ results. With $d\kappa_1/d\lambda_1$ according to equation (69) one obtains from equation (70) after division by $2g$ since the latter does not disappear in the range $0 \leq \lambda_1 \leq 1$:

$$\lambda_1 \left(g + \lambda_1 \frac{dg}{d\lambda_1} \right) \frac{d\lambda_1}{d\xi} = (1 - \lambda_1) \frac{\frac{6}{\pi} - c\lambda_1}{1 - c\lambda_1} \quad (71)$$

$$\text{Initial value: } \xi = 0: \lambda_1 = 0 \quad (71a)$$

Because of $g(0, 0) = p_0 = \frac{6}{\pi} - \frac{3}{2}$ one obtains from it in the neighbourhood of $\xi = 0$, $\lambda_1 = 0$:

$$\frac{d\xi}{d\lambda_1} = \frac{6}{\pi} p_0 \lambda_1 = \frac{6}{\pi} \left(\frac{6}{\pi} - \frac{3}{2} \right) \lambda_1 \quad (72)$$

and

$$\xi = \frac{3}{\pi} \left(\frac{6}{\pi} - \frac{3}{2} \right) \lambda_1^2 = 0.391 \lambda_1^2 \quad (73)$$

Hence follows for the neighborhood of the leading edge of the plate ($\xi = 0$)

$$\lambda_1 = 1.60 \sqrt{\xi} \quad \text{or} \quad \frac{-v_o \delta_1}{v} = 1.60 \sqrt{\xi}$$

Because of $\frac{\delta^*}{\delta_1} = 3 - \frac{6}{\pi}$ follows hence:

$$\frac{-v_o \delta^*}{v} = (\pi - 2) \sqrt{\frac{2}{4 - \pi}} \sqrt{\xi}$$

or

$$\delta^* = (\pi - 2) \sqrt{\frac{2}{4 - \pi}} \sqrt{\frac{U_o}{U}}$$

As the comparison with equation (51) shows, the boundary layer thickness starts, therefore, at the leading edge of the plate with the value for the plate without suction.

In order to integrate the equation (71), one has to insert the explicit values of $g(\lambda_1)$ and $dg/d\lambda_1$ according to equation (62). After some intermediate calculating (compare appendix I) one obtains

$$\frac{d\xi}{d\lambda_1} = \frac{\lambda_1 (P_0 + P_1 \lambda_1 + P_2 \lambda_1^2 + P_3 \lambda_1^3)}{(1 - c\lambda_1)^2 (1 - \lambda_1) \left(\frac{\pi}{6} - c\lambda_1 \right)} \quad (74)$$

with

$$\left. \begin{aligned} P_0 &= p_0 = 0.40986 \\ P_1 &= 2p_1 + p_0 c = -0.4667 \\ P_2 &= 3p_2 = 0.17457 \\ P_3 &= -cp_2 = -0.02772 \end{aligned} \right\} \quad (75)$$

The breaking up into partial fractions yields:

$$\frac{d\xi}{d\lambda_1} = \frac{P_3}{c^3} + \frac{K_1}{\lambda_1 - 1} + \frac{K_2}{c\lambda_1 - \frac{\pi}{6}} + \frac{K_3}{(c\lambda_1 - 1)^2} + \frac{K_4}{c\lambda_1 - 1} = f'(\lambda_1) \quad (76)$$

The integration with the initial value $\lambda_1 = 0$ for $\xi = 0$ yields

$$\begin{aligned} \xi = & \frac{P_3}{c^3} \lambda_1 + K_1 \ln(1 - \lambda_1) + \frac{K_2}{c} \ln\left(1 - \frac{6c}{\pi} \lambda_1\right) \\ & - K_3 \frac{\lambda_1}{c\lambda_1 - 1} + \frac{K_4}{c} \ln(1 - c\lambda_1) = f(\lambda_1) \end{aligned} \quad (77)^2$$

The K_1, \dots, K_4 result from the breaking up into partial fractions as

$$K_1 = -6.9560; \quad K_2 = 3.4704; \quad K_3 = -0.2284; \quad K_4 = -0.1569 \quad (78)$$

Thus the solution finally reads

$$\begin{aligned} \xi = & -0.2564\lambda_1 - 6.956 \ln(1 - \lambda_1) + 7.2846 \ln(1 - 0.9099\lambda_1) \\ & + 0.2284 \frac{\lambda_1}{0.4764\lambda_1 - 1} - 0.3293 \ln(1 - 0.4764\lambda_1) \end{aligned} \quad (79)$$

²For development of this solution in the neighborhood of $\xi = 0$, $\lambda_1 = 0$, the coefficient of λ_1 must, because of equation (73), equal zero; the coefficient of λ_1^2 must equal $\frac{3}{\pi} \left(\frac{6}{\pi} - \frac{3}{2} \right) = 0.391$. The result is:

$$\frac{P_3}{c^3} - K_1 - \frac{6}{\pi} K_2 + K_3 - K_4 = 0 \quad (77a)$$

$$- \frac{K_1}{2} - \frac{18c}{\pi^2} K_2 + cK_3 - \frac{c}{2} K_4 = \frac{3}{\pi} \left(\frac{6}{\pi} - \frac{3}{2} \right) \quad (77b)$$

With the numerical values of equation (78) one may verify that these equations are satisfied.

The solution $\lambda_1(\xi)$ calculated accordingly is given in table 5.

From $\lambda_1(\xi)$ all remaining boundary layer parameters can then be calculated immediately according to equations (61), (62), (63), and (64). They also are

given in table 5. In figure 9 $\frac{-v_0 \delta^*}{\nu}$, $\frac{\delta^*}{\delta}$ and $\frac{\tau_0 \delta^*}{\mu U_0}$ are plotted against $\sqrt{\xi}$.

The displacement thickness of the boundary layer reaches 0.95 of its asymptotic value after an extent of the growing boundary layer of

$\xi_A = \left(\frac{v_0}{U_0} \right)^2 \frac{U_0 x_A}{\nu} \approx 4.5$. The velocity profiles in the growing boundary

layer in the plotting u/U_0 against $\frac{-v_0 y}{\nu} = \eta \lambda_1$ are represented in figure 10. For the wall shearing stress one obtains from equations (64) and (4a):

$$\frac{\tau_0}{\tau_{0\infty}} = \frac{\frac{\pi}{6}}{\lambda_1(1 - c\lambda_1)} \quad (80)$$

The wall shearing stress is plotted in figure 11 as a function of $\sqrt{\xi}$.

Drag. - In view of the reduction of the drag by maintenance of a laminar boundary layer the friction drag in the extent of growing boundary layer is of particular interest for this solution. For the asymptotic solution the local friction drag along the wall is constant with $\tau_{0\infty} = -\rho v_0 U_0$; thus the coefficient of the total friction drag also equals this value

$$c_{f\infty} = \frac{W}{\frac{\rho}{2} U_0^2 b l} = \frac{\tau_{0\infty}}{\frac{\rho}{2} U_0^2} = -2 \frac{v_0}{U_0} \quad (81)$$

For small suction quantities $-v_0/U_0$ the extent of growing boundary layer is sometimes so large that the growth is not finished by far at the end of the plate. According to former investigations (references 8 and 10) it is to be expected that for homogeneous suction at the plate the maintenance of a laminar boundary layer is possible even for Reynolds

numbers of the order of magnitude $\frac{U_0 l}{\nu} = 10^7$ to 10^8 with a very small suction quantity of the order of magnitude $c_Q = \frac{-v_0}{U_0} = 10^{-4}$. For $\frac{-v_0}{U_0} = 10^{-4}$ and $\frac{U_0 l}{\nu} = 10^7$ or 10^8 one has at the end of the plate

$\xi_l = \left(\frac{v_0}{U_0} \right)^2 \frac{U_0 l}{\nu} = 0.1$ or 1, that is, the growth of the boundary layer is not finished by far.

Since the friction layer over the extent of growing boundary layer is thinner, the friction drag there is considerably larger than for the asymptotic solution. For this reason the calculation of the drag over the extent of growing boundary layer will be given completely.

The total friction drag for the plate wetted on one side is:

$$W = b \int_0^l \tau_0 \, dx \quad (82)$$

and with the value of τ_0 according to equation (80) and with $\tau_{0\infty}$ according to equation (4a):

$$W = -\rho v_0 U_0 b \frac{\pi}{6} \int_0^l \frac{dx}{\lambda_1(1 - c\lambda_1)}$$

With $dx = \left(\frac{U_0}{v_0}\right)^2 \frac{v}{U_0} d\xi$ according to equation (67) this equation becomes:

$$W = \rho b U_0^2 \frac{v}{-v_0} \frac{\pi}{6} \int_{\xi=0}^{\xi_l} \frac{d\xi}{\lambda_1(1 - c\lambda_1)} \quad (83)$$

with ξ_l signifying the value of ξ at the end of the plate, thus:

$$\xi_l = \left(\frac{v_0}{U_0}\right)^2 \frac{U_0 l}{v} = f(\lambda_{10}) \quad (84)$$

Therein λ_{10} signifies the value of λ_1 at the end of the plate which is obtained from equation (77) for $\xi = \xi_l$; therefore

$$\begin{aligned} f(\lambda_{10}) = & \frac{P_3}{c^3} \lambda_{10} + K_1 \ln(1 - \lambda_{10}) + \frac{K_2}{c} \ln\left(1 - \frac{6c}{\pi} \lambda_{10}\right) \\ & - K_3 \frac{\lambda_{10}}{c\lambda_{10} - 1} + \frac{K_4}{c} \ln(1 - c\lambda_{10}) \end{aligned} \quad (85)$$

Introducing in equation (83) for $\frac{d\xi}{d\lambda_1} = f'(\lambda_1)$ the expression according to equation (76) one obtains:

$$W = \rho b U_o^2 \frac{v}{-v_o} F(\lambda_{lo})$$

and

$$c_f = \frac{W}{\frac{\rho}{2} U_o^2 b l} = 2 \frac{v}{-v_o l} F(\lambda_{lo}) \quad (86)$$

with $F(\lambda_{lo})$ signifying

$$F(\lambda_{lo}) = \frac{\pi}{6} \int_{\lambda_1=0}^{\lambda_{lo}} \frac{f'(\lambda_1) d\lambda_1}{\lambda_1(1 - \alpha\lambda_1)} \quad (87)$$

Finally introducing $\frac{v}{-v_o l} = \frac{-v_o}{U_o} f(\lambda_{lo})$ according to equation (84) into equation (86) one obtains

$$c_f = 2 \frac{-v_o}{U_o} \frac{F(\lambda_{lo})}{F(\lambda_{lo})} = 2 \frac{-v_o}{U_o} G(\lambda_{lo})$$

or

$$c_f = c_{f_\infty} G(\lambda_{lo}) \quad (88)$$

Because of the connection between λ_{lo} and ξ_l according to equation (84), the total drag coefficient for the extent of growing boundary layer is thereby given as a function of the dimensionless distance along the plate $\xi_l = \left(\frac{v_o}{U_o}\right)^2 \frac{U_o x}{v}$. On the other hand, equations (84)

and (88) give for prescribed mass coefficient of the suction $-v_0/U_0$ the drag law of c_f also against $U_0 l/v$ in the form of a parameter representation. The parameter λ_{10} is the dimensionless boundary layer thickness at the end of the plate: $\lambda_{10} = \left(\frac{-v_0 \delta_1}{v} \right)_{x=l}$. The values of λ_{10} lie between 0 and 1, the first value being valid at the leading edge of the plate, the latter for the asymptotic solution, after the growth of the boundary layer has ended.

The calculation of the integral $F(\lambda_{10})$ according to equation (87) gives (appendix II)

$$\begin{aligned}
 \frac{6}{\pi} F(\lambda_{10}) = & \left(-\frac{p_3}{c^3} - \frac{K_1 c}{1-c} - \frac{K_2}{c} - K_3 + K_4 \right) \ln(1 - c\lambda_{10}) \\
 & + \frac{6}{\pi K_1} \ln(1 - \lambda_{10}) + \frac{6}{\pi c} K_2 \ln \left(1 - \frac{6c}{\pi} \lambda_{10} \right) \\
 & - (-K_3 + K_4) \frac{c\lambda_{10}}{1 - c\lambda_{10}} + \frac{K_3}{2} \frac{c\lambda_{10}(2 - c\lambda_{10})}{(1 - c\lambda_{10})^2} \quad (89)
 \end{aligned}$$

c is, according to equation (60), $c = 1 - \frac{\pi}{6}$, and K_1, \dots, K_4 are given by equations (75) and (78). After insertion of the numerical values according to equations (60) and (78) follows:

$$\begin{aligned}
 F(\lambda_{10}) = & -0.3288 \ln(1 - 0.4764\lambda_{10}) - 6.956 \ln(1 - \lambda_{10}) \\
 & + 7.2846 \ln(1 - 0.9099\lambda_{10}) \\
 & - 0.0374 \frac{0.4764\lambda_{10}}{1 - 0.4764\lambda_{10}} - 0.05980 \frac{0.4764\lambda_{10}(2 - 0.4764\lambda_{10})}{(1 - 0.4764\lambda_{10})^2}
 \end{aligned}$$

The values of $F(\lambda_{10})$ and $G(\lambda_{10})$ are given in table 6. For $\lambda_{10} \rightarrow 1$ that is $\xi \rightarrow \infty$ (growth of boundary layer ended) one has, as can immediately be seen from equations (89) and (77):

$$\lambda_{lo} \rightarrow 1: \frac{F(\lambda_{lo})}{f(\lambda_{lo})} = G(\lambda_{lo}) = 1 \quad (89a)$$

and thus $c_f \rightarrow c_{f\infty}$ for $\xi_l \rightarrow \infty$. On the other hand one has in the neighborhood of the leading edge of the plate, that is, for $\lambda_{lo} \rightarrow 0$ according to equation (73)

$$\lambda_{lo} \rightarrow 0: f(\lambda_{lo}) = \frac{3}{\pi} \left(\frac{6}{\pi} - \frac{3}{2} \right) \lambda_{lo}^2$$

and thus according to equation (87)

$$\lambda_{lo} \rightarrow 0: F(\lambda_{lo}) = \left(\frac{6}{\pi} - \frac{3}{2} \right) \lambda_{lo}$$

and therefore

$$\lambda_{lo} \rightarrow 0: G(\lambda_{lo}) = \frac{\pi}{3} \frac{1}{\lambda_{lo}} \quad (89b)$$

If one substitutes this value into equation (88) and takes into consideration that

$$\lambda_{lo} = \sqrt{\xi_l} \frac{1}{\sqrt{\frac{3}{\pi} \left(\frac{6}{\pi} - \frac{3}{2} \right)}}$$

is valid for small λ_{lo} according to equation (73), one obtains

$$c_f = 2 \frac{-v_o}{U_o} \sqrt{\frac{4 - \pi}{2}} \sqrt{\xi_l}$$

or

$$c_f = \sqrt{8 - 2\pi} \left(\frac{U_0 l}{v} \right)^{-1/2}$$

thus the drag law of the plate without suction according to equation (52). The drag law of the length of growing boundary layer is therefore for very small lengths of growing boundary ξ_l asymptotically transformed into the drag law of the plate without suction.

The drag law according to equation (88) is represented in figure 12, where $c_f/c_{f\infty}$ is plotted against ξ_l . Furthermore figure 13 gives the drag law in the form c_f against $U_0 l/v$ for various values of the mass coefficient $-v_0/U_0$. The larger the suction quantity the smaller the Reynolds number at which the respective c_f - curve separates from the drag curve of the plate without suction and is transformed, after a certain transition region, into the asymptotic curve $c_{f\infty} = \frac{-2v_0}{U_0}$. The Reynolds number at which the latter is reached is the larger, the smaller the suction quantity.

The drag coefficients given here represent the total drag of the plate with suction. No special sink drag is added (compare reference 10) since for continuous suction, as in the present case, the sucked particles of fluid have already given up their entire x -momentum in the boundary layer so that this momentum is contained in the friction drag.

In order to obtain the total drag power of the plate with suction, however, one must, aside from the drag given here, take into account the blower power of the suction.

(b) The Plate Stagnation Point Flow with Homogeneous Suction

Another special case which can be solved in closed form is the plane stagnation point flow with homogeneous suction. Since for this case the exact solution from the differential equations of the boundary layer has been given elsewhere (reference 9) it shall also briefly be treated here. The potential flow is $U(x) = u_1 x$ and the suction velocity $v_0(x) = v_0(0) = v_{00} < 0$. If the integral curve of equation (28) is to have a finite value at the stagnation point $x = 0$, there has to be $G(\kappa, \kappa_1) = 0$; this in turn requires, as was discussed in detail in chapter IV c, $F(\lambda, \lambda_1) = 0$. $F(\lambda, \lambda_1)$ is given by equation (33). The values of λ_0, λ_{10} which belong together follow from it; they give for the general case the initial values of the boundary layer calculation at the stagnation point; for the present case of stagnation point flow they

immediately give the complete solution since the boundary layer thickness and all other parameters are independent of the length of growing boundary layer x . Besides λ_1 , λ one further obtains K according to equation (14), g according to equation (17), δ^*/ϑ according to equation (19), and κ_0 and κ_{10} according to equation (31). The mass coefficient $C_0 = \frac{-v_{00}}{\sqrt{U_0'v}}$ is obtained according to equation (34). From κ_0 finally follows ϑ and therewith δ^* . The results are compiled in table 4. Naturally, momentum and displacement thickness decrease with increasing suction quantity. With $C_0 \rightarrow \infty$ the form parameter δ^*/ϑ approaches the value 2 of the asymptotic suction profile. In figure 14 $\vartheta \sqrt{u_1/v}$ and $\delta^* \sqrt{u_1/v}$ are plotted against C_0 and compared with the exact solution. The agreement is quite satisfactory.

As conclusion of these considerations of the special cases the characteristic boundary layer parameters for these special cases are compiled in the following table.

Boundary Layer Parameters for Various Special Cases

Case	K	λ	λ_1	κ	κ_1	$\frac{\delta^*}{\delta_1}$	$\frac{\delta}{\delta_1} = g$	$\frac{\delta^*}{\delta}$
Plate without suction	-1	0	0	0	0	1.089	0.410	2.66
Stagnation point flow without suction	-0.6453	0.3547	0	0.0709	0	1.058	0.447	2.37
(Separation point calculated)	-2.099	-1.099 for all λ_1	$f(c_Q)$	-0.0721	$f(c_Q)$	1.189	0.256	4.64
Separation point according to Hartree	$f(\lambda, \lambda_1)$	$f(\lambda_1)$	$f(c_Q)$	-0.0682	$f(c_Q)$	$f(c_Q)$	$f(c_Q)$	4.03
Asymptotic suction profile	0	0	1	0	$\frac{1}{2}$	1	$\frac{1}{2}$	2

V I. E X A M P L E S ³

In this section the new method shall be tried on a few more examples.

(a) Circular Cylinder

As first example the circular cylinder with homogeneous suction has been calculated for various suction quantities C_0 . The results (displacement thickness δ^* and form parameter κ)

³ The numerical calculations of this section have been carried out by Mr. A. Ulrich.

are given in figure 15. For the case without suction $\phi = 101.7^\circ$ results as separation point; this is slightly further to the front than for the customary Pohlhausen method ($\phi = 108.9^\circ$) for which the calculation was performed elsewhere (reference 7). With increasing suction quantity results a reduction of the boundary layer thickness and a shifting of the separation point toward the rear.

In order to completely avoid the separation for the circular cylinder, it is probably useful to select not a homogeneous suction along the contour, as in the present case, but a distribution of $v_0(x)$ which has considerably larger values on the rear than on the foreside. Such calculations may also be carried out according to the present method without additional expenditure of time.

A comparison of the present approximate calculation with an exact calculation by K. Bussmann (reference 17) for the displacement and momentum thickness is given in figure 16. The latter calculation is a development in power series starting from the stagnation point, as first indicated by Blasius (reference 11). Except for the neighborhood of the separation point the agreement is quite satisfactory.

(b) Symmetrical Joukowsky Profiles for $c_a = 0$

As second example a symmetrical Joukowsky profile of 15 percent thickness has been calculated for $c_a = 0$, also with homogeneous suction. The suction extends over the entire contour. The same profile without suction has been calculated elsewhere (reference 7), also according to the Pohlhausen method. Here, too, a reduction of the boundary layer thickness and a shifting of the separation point toward the rear results with increasing suction quantity. For the suction quantity $C_0 = 0.417$, that is $f_1(0) = 3$, a separation does no longer occur.

V I I. S U M M A R Y

A method of approximation for calculation of the laminar boundary layer with suction for arbitrary body contour and arbitrary distribution of the suction quantity along the contour of the body in the flow is developed. The method is related to the well-known Pohlhausen method for calculation of the laminar boundary layer without suction. The calculation requires the integration of a differential equation of the first order according to the isocline method. The method is applied to several special cases for which there also exist, in part, exact solutions: Plate in longitudinal flow and plane stagnation point flow with homogeneous suction. Furthermore the circular cylinder and symmetrical Joukowsky profile with homogeneous suction were calculated as examples.

V I I I. A P P E N D I X E S

APPENDIX I

Concerning the Length of Growing Boundary Layer for the Plane Plate
with Homogeneous Suction

According to equation (71) is

$$\lambda_1 \left(g + \lambda_1 \frac{dg}{d\lambda_1} \right) \frac{d\lambda_1}{d\xi} = (1 - \lambda_1) \frac{\frac{\pi}{6} - c\lambda_1}{1 - c\lambda_1} \quad (71)$$

From equation (62) one finds:

$$\begin{aligned} \frac{dg}{d\lambda_1} &= \frac{(1 - c\lambda_1)(p_1 + 2p_2\lambda_1) + 2c(1 - c\lambda_1)(p_0 + p_1\lambda_1 + p_2\lambda_1^2)}{(1 - c\lambda_1)^4} \\ &= \frac{p_1 + 2cp_0 + (p_1c + 2p_2)\lambda_1}{(1 - c\lambda_1)^3} \end{aligned} \quad (I,1)$$

Substitution of equations (I,1) and (62) into equation (71) gives:

$$\lambda_1 \left[\frac{p_0 + p_1 \lambda_1 + p_2 \lambda_1^2}{(1 - c \lambda_1)^2} + \lambda_1 \frac{p_1 + 2c p_0 + (p_1 c + 2p_2) \lambda_1}{(1 - c \lambda_1)^3} \right] = (1 - \lambda_1) \frac{\frac{\pi}{6} - c \lambda_1}{1 - c \lambda_1} \frac{d \xi}{d \lambda_1}$$

and after multiplication by $(1 - c \lambda_1)$:

$$\lambda_1 \left[\frac{(p_0 + p_1 \lambda_1 + p_2 \lambda_1^2)(1 - c \lambda_1) + \lambda_1(p_1 + 2c p_0) + \lambda_1^2(p_1 c + 2p_2)}{(1 - c \lambda_1)^2} \right] = (1 - \lambda_1) \left(\frac{\pi}{6} - c \lambda_1 \right) \frac{d \xi}{d \lambda_1} \quad (I,2)$$

$$\frac{\lambda_1}{(1 - c \lambda_1)^2} \left[p_0 + (2p_1 + cp_0)\lambda_1 + 3p_2\lambda_1^2 - cp_2\lambda_1^3 \right] = (1 - \lambda_1) \left(\frac{\pi}{6} - c \lambda_1 \right) \frac{d \xi}{d \lambda_1}$$

$$\frac{d \xi}{d \lambda_1} = \frac{\lambda_1(p_0 + p_1 \lambda_1 + p_2 \lambda_1^2 + p_3 \lambda_1^3)}{(1 - c \lambda_1)^2 (1 - \lambda_1) \left(\frac{\pi}{6} - c \lambda_1 \right)} \quad (74)$$

with

$$\left. \begin{array}{l} p_0 = p_0; \quad p_1 = 2p_1 + cp_0; \\ p_2 = 3p_2; \quad p_3 = -cp_2 \end{array} \right\} \quad (75)$$

APPENDIX II

Concerning the Calculation of the Drag of the Plane Plate
with Homogeneous Suction

The calculation of

$$F(\lambda_{10}) = \frac{\pi}{6} \int_{\lambda_1=0}^{\lambda_{10}} \frac{f'(\lambda_1) d\lambda_1}{\lambda_1(1 - c\lambda_1)} \quad (87)$$

gives with $f'(\lambda_1)$ according to equation (76), if λ_1 is replaced by z ,

$$\begin{aligned} \frac{6}{\pi} F(\lambda_{10}) &= \frac{P_3}{c^3} \int_{z=0}^{\lambda_{10}} \frac{dz}{z(1 - cz)} + K_1 \int_{z=0}^{\lambda_{10}} \frac{dz}{(z - 1)z(1 - cz)} \\ &+ K_2 \int_{z=0}^{\lambda_{10}} \frac{dz}{(cz - \frac{\pi}{6})z(1 - cz)} + K_3 \int_{z=0}^{\lambda_{10}} \frac{dz}{(cz - 1)^2 z(1 - cz)} \\ &- K_4 \int_{z=0}^{\lambda_{10}} \frac{dz}{(cz - 1)^2 z} = I + II + III + IV + V \quad (II,1) \end{aligned}$$

The integrals are solved by breaking up into partial fractions. One finds:

$$I = \frac{P_3}{c^3} \left[\ln z - \ln \left(z - \frac{1}{c} \right) \right]_{z=0}^{\lambda_{10}}$$

$$II = -K_1 \left[\ln z + \frac{1}{c-1} \ln (z-1) + \frac{c}{1-c} \ln \left(z - \frac{1}{c} \right) \right]_{z=0}^{\lambda_{10}}$$

$$III = -K_2 \left[\frac{6}{\pi} \ln z + \frac{1}{c} \ln \left(z - \frac{1}{c} \right) - \frac{6}{\pi c} \ln \left(z - \frac{\pi}{6c} \right) \right]_{z=0}^{\lambda_{10}}$$

$$IV = K_3 \left[\ln z - \ln(cz - 1) - \frac{1}{cz - 1} + \frac{1}{2} \frac{1}{(cz - 1)^2} \right]_0^{\lambda_{10}}$$

$$V = K_4 \left[-\ln z + \frac{1}{cz - 1} + \ln(cz - 1) \right]_0^{\lambda_{10}}$$

When summed up, all terms with $[\ln z]_0^{\lambda_{10}}$ cancel each other, because of equation (77a). After insertion of the limits the remaining terms give:

$$[\ln(cz - 1)]_0^{\lambda_{10}} = \ln(1 - c\lambda_{10}); \quad [\ln(z - 1)]_0^{\lambda_{10}} = \ln(1 - \lambda_{10})$$

$$[\ln z - \frac{\pi}{6c}]_0^{\lambda_{10}} = \ln \left(1 - \frac{6c}{\pi} \lambda_{10} \right); \quad \left[\frac{1}{cz - 1} \right]_0^{\lambda_{10}} = \frac{-c\lambda_{10}}{1 - c\lambda_{10}}$$

$$\left[\frac{1}{(cz - 1)^2} \right]_0^{\lambda_{10}} = \frac{c\lambda_{10}(2 - c\lambda_{10})}{(1 - c\lambda_{10})^2}$$

Thus there results by simplification from equation (II,1):

$$\begin{aligned}
 \frac{6}{\pi} F(\lambda_{10}) &= \left(-\frac{P_3}{c^3} - \frac{K_1 c}{1-c} - \frac{K_2}{c} - K_3 + K_4 \right) \ln(1 - c\lambda_{10}) \\
 &+ \frac{6}{\pi K_1} \ln(1 - \lambda_{10}) + \frac{6}{\pi c K_2} \ln\left(1 - \frac{6c}{\pi} \lambda_{10}\right) \\
 &- (-K_3 + K_4) \frac{c\lambda_{10}}{1 - c\lambda_{10}} + \frac{K_3}{2} \frac{c\lambda_{10}(2 - c\lambda_{10})}{(1 - c\lambda_{10})^2} \quad (89)
 \end{aligned}$$

APPENDIX III

To page 30. - Table 10 gives the numerical table concerning the velocity distribution of figure 10.

To page 35. - For the boundary on the plate in longitudinal flow with homogeneous suction the exact solution from the differential equations also was given in an unpublished report by Iglisch. A comparison of the approximate solution above with that exact solution is given in figures 18 and 19. Figure 18 gives the comparison of the displacement and momentum thickness; particularly for the displacement thickness the agreement is good. Figure 19 gives the comparison for the wall shearing stress; here also the agreement is satisfactory. (So far, these comparisons can be carried out only for the front part of the length of growing boundary layer, up to $\xi = 0.5$, since the exact solution does not yet completely exist.)

R E F E R E N C E S

1. Betz, A.: Beeinflussung der Grenzschicht und ihre praktische Verwertung. *Jahrb. Dtsch. Akad. Luftfahrtforschung* 1939/40, p. 246 and *Schriften d. Dtsch. Akad. Luftfahrtforschung* Heft 49 (1942).
2. Holstein, H.: Messungen zur Laminarhaltung der Grenzschicht durch Absaugung an einem Tragflügel. *Bericht S. 10 der Lilienthal-Gesellschaft für Luftfahrtforschung* 1942.
3. Holstein, H.: Messungen zur Laminarhaltung der Reibungsschicht durch Absaugung an einem Tragflügel mit Profil NACA 0012-64, *FB 1654*, 1942.
4. Ackeret, J., Ras, M., and Pfenninger, W.: Verhinderung des Turbulenzwerdens einer Reibungsschicht durch Absaugung. *Die Naturwissenschaften* 1941, p. 622.
5. Schlichting, H.: Die Grenzschicht mit Absaugung und Ausblasen. *Luftfahrtforschung* Bd. 19, p. 179 (1942).
6. Schlichting, H.: Die Grenzschicht an der ebenen Platte mit Absaugung und Ausblasen. *Luftfahrtforschung* Bd. 19, p. 293 (1942).
7. Schlichting, H., and Ulrich, A.: Zur Berechnung des Umschlages laminar/turbulent. *Bericht S. 10 der Lilienthal-Gesellschaft für Luftfahrtforschung*, p. 75, 1942 and *Jahrb. 1942 der Dtsch. Luftfahrtforschung*, p. I 8.
8. Bussmann, K., and Münz, H.: Über die Stabilität der laminaren Reibungsschicht. *Jahrb. 1942 der dtsch. Luftfahrtforschung*, p. I 36.
9. Schlichting, H., and Bussmann, K.: Exakte Lösungen für die laminare Grenzschicht mit Absaugen und Ausblasen. *Schriften der Dtsch. Akad. d. Luftfahrtforschung*, 1943.
10. Schlichting, H.: Die Beeinflussung der Grenzschicht durch Absaugen und Ausblasen. Lecture to the Deutschen Akademie der Luftfahrtforschung May 7, 1943; to be published soon.
11. Blasius, H.: Grenzschichten in Flüssigkeiten mit kleiner Reibung. *Zschr. Math. u. Phys.*, Bd. 56, p. 1 (1908).
12. Hiemenz, K.: Die Grenzschicht an einem in den gleichmässigen Flüssigkeitsstrom eingetauchten Kreiszylinder. *Dingl. Polytechn. Journal*. Bd. 326, p. 321 (1911).

13. Hartree, D. R.: On an Equation Occurring in Falkner and Skan's Approximate Treatment of the Equations of the Boundary Layer. Cambridge Phil. Soc. Vol. 33, p. 223 (1937).
14. Howarth, L.: On the Solution of the Laminar Boundary Layer Equations. Proc. Roy. Soc. London A No. 919, Vol. 164 (1938), p. 547.
15. Pohlhausen, K.: Zur näherungsweisen Integration der Differentialgleichung der laminaren Grenzschicht. Zschr. angew. Math. u. Mech. Bd. 1, p. 252 (1921).
16. Ulrich, A.: Die Stabilität der laminaren Reibungsschicht an der längsangeströmten Platte mit Absaugung und Ausblasen. Bericht 43/9 des Aerodynamischen Instituts der T. H. Braunschweig; to be published soon.
17. Bussmann, K.: Exakte Lösungen für die Grenzschicht am Kreiszylinder mit Absaugen und Ausblasen. Not published.
18. Prandtl, L.: The Mechanics of Viscous Fluids. Durand, Aerodynamic Theory vol. III, Berlin 1935.
19. Holstein, H., and Bohlen, T.: Ein vereinfachtes Verfahren zur Berechnung laminarer Reibungsschichten, die dem Ansatz von K. Pohlhausen genügen. Bericht S. 10 der Lilienthal-Gesellschaft für Luftfahrtforschung 1942.
20. Iglisch, R.: Über das asymptotische Verhalten der Lösungen einer nichtlinearen gewöhnlichen Differentialgleichung 3. Ordnung. Bericht 43/14 des Aerodynamischen Instituts der T. H. Braunschweig; to be published soon.

TABLE 1
 THE BASIC FUNCTIONS F_1 AND F_2
 FOR THE VELOCITY DISTRIBUTION
 IN THE BOUNDARY LAYER
 WITH SUCTION

$\eta = \frac{y}{\delta_1}$	F_1	F_2
0	0	0
.2	.1813	.0768
.4	.3297	.1221
.6	.4512	.1423
.8	.5507	.1452
1.0	.6321	.1322
1.2	.6988	.1112
1.4	.7534	.0843
1.6	.7981	.0551
1.8	.8347	.0263
2.0	.8647	-.0017
2.2	.8892	-.0240
2.4	.9093	-.0416
2.6	.9257	-.0524
2.8	.9392	-.0552
3.0	.9502	-.0498
3.5	.9698	-.0302
4.0	.9817	-.0183
4.5	.9889	-.0111
5.0	.9933	-.0067
6.0	.9975	-.0025
7.0	.9991	-.0009
∞	1	0

TABLE 2
PARAMETER OF BOUNDARY LAYER WITH SUCTION

$-K$	$g = \frac{\vartheta}{\delta_1}$	$g^* = \frac{\delta^*}{\delta_1}$	$\frac{\delta^*}{\vartheta}$	$\frac{\tau_0 \delta_1}{\mu U}$	$\frac{\tau_0 \vartheta}{\mu U}$
a 0	0.5	1	2	1	0.5
	.4931	1.009	2.05	.9524	.4696
	.4856	1.018	2.10	.9047	.4393
	.4779	1.027	2.15	.8571	.4096
	.4696	1.036	2.21	.8094	.3801
b .6453	.5	1.045	2.27	.7618	.3510
	.6	1.054	2.33	.7142	.3225
	.6453	1.058	2.37	.6926	.3097
	.7	1.063	2.41	.6665	.2945
	.8	1.072	2.48	.6189	.2672
c 1.0	.9	1.081	2.57	.5712	.2405
	1.0	1.090	2.66	.5236	.2146
	1.1	1.099	2.76	.4760	.1895
	1.2	1.108	2.87	.4283	.1654
	1.3	1.117	2.99	.3807	.1461
	1.4	1.126	3.12	.3330	.1201
	1.5	1.135	3.27	.2854	.0991
	1.6	1.144	3.43	.2378	.0792
	1.7	1.153	3.62	.1901	.0606
	1.8	1.162	3.82	.1425	.0433
d 2.099	1.9	1.171	4.09	.0948	.0273
	2.0	1.180	4.33	.0472	.0129
	2.099	1.189	4.64	0	0

^aAsymptotic suction profile.

^bStagnation point without suction.

^cPlane plate without suction.

^dSeparation point.

TABLE 3

THE FUNCTION $G(\kappa, \kappa_1)$ FOR THE INTEGRATION
 OF THE DIFFERENTIAL EQUATION
 OF THE MOMENTUM THICKNESS

$\kappa_1 = 0$ without suction				$\kappa_1 = 0.1$			
λ	λ_1	κ	$G(\kappa, \kappa_1)$	λ	λ_1	κ	$G(\kappa, \kappa_1)$
0.50	0	0.1062	-0.2042	0.5	0.206	0.1132	-0.333
.45		.0937	-.1323	.4	.210	.0875	-.192
.40		.0816	-.0621	.3	.215	.0627	-.057
.3547		.0709	0	0		.0520	0
.30		.0586	.0729	.2	.221	.0401	.072
.25		.0477	.1375	.1	.227	.0190	.190
.20		.0373	.2001	0	.235	0	.300
.15		.0273	.2607	-.2	.250	-.0330	.490
.10		.0177	.3191	-.4	.270	-.0550	.635
.05		.0086	.3753	-.6	.290	-.0710	.742
0		0	.4292	-.8	.320	-.0775	.792
				-1.099		-.0721	.758
$\kappa_1 = 0.2$							
λ	λ_1	κ	G	λ	λ_1	κ	G
-.5		.0602	.8330	0.5	0.405	0.1213	-0.450
-.6		.0666	.8820	.4	.415	.0936	-.310
-.7		.0711	.9198	.3	.424	.0674	-.172
-.8		.0738	.9470	.2	.432	.0431	-.095
-.9		.0748	.9617			.0350	0
-1.0		.0742	.9656	.1	.443	.0205	.077
-1.099	↓	.0721	.9584	0	.454	0	.188
		-.0682		-.2	.480	-.0355	.370
				-.4	.515	-.0590	.516
				-.6	.557	-.0770	.620
				-.8	.620	-.0835	.657
				-1.099		-.0721	.558

A

TABLE 3 - Concluded

THE FUNCTION $G(\kappa, \kappa_1)$ FOR THE INTEGRATION

OF THE DIFFERENTIAL EQUATION OF THE

MOMENTUM THICKNESS - Concluded

$\kappa_1 = 0.3$				$\kappa_1 = 0.5$			
λ	λ_1	κ	$G(\kappa, \kappa_1)$	λ	λ_1	κ	$G(\kappa, \kappa_1)$
0.5	0.590	0.1292	-0.542	0.4	0.935	0.113	-0.475
.4	.600	.100	-.400	.3	.950	.0825	-.350
.3	.611	.0722	-.265	.2	.965	.0538	-.225
.2	.622	.0463	-.136	.1	.982	.0220	-.100
.1	.637	.0222	-.016	0	1.0	0	0
0	.652	0	.099	-.2	1.045	-.0460	.195
-.2	.688	-.0380	.294	-.4	1.115	-.0810	.320
-.4	.738	-.0660	.438	-1.099		-.0721	-.042
-.6	.808	-.0830	.520				
-.8	.892	-.0910	.555				
-1.099	1.172	-.0721	.358				
$\kappa_1 = 0.4$				$\kappa_1 = 0.6$			
λ	λ_1	κ	$G(\kappa, \kappa_1)$	λ	λ_1	κ	$G(\kappa, \kappa_1)$
0.4	0.770	0.1068	-0.460	0.3	1.116	0.088	-0.327
.3	.782	.0777	-.324	.2	1.122	.056	-.206
.2	.800	.0500	-.200	.1	1.135	.020	-.072
.1	.815	.0202	-.080	0	1.154	0	0
		.008	0	-.2	1.200	-.048	.190
0	.835	0	.035	-.4	1.254	-.086	.340
-.2	.875	-.0415	.232				
-.4	.935	-.0730	.375				
-1.099		-.0721	.158				
$\kappa_1 = 0.7$				$\kappa_1 = 0.7$			
λ	λ_1	κ	$G(\kappa, \kappa_1)$	λ	λ_1	κ	$G(\kappa, \kappa_1)$
0.3	1.294	0.089	-0.125	0.3	1.294	0.089	-0.125
.2	1.292	.059	-.082	.2	1.292	.059	-.082
.1	1.296	.030	-.005	.1	1.296	.030	-.005
0	1.304	0	.089	0	1.304	0	.089
-.2	1.338	-.054	.262	-.2	1.338	-.054	.262
-.4	1.401	-.096	.402	-.4	1.401	-.096	.402

TABLE 4

INITIAL VALUES OF THE PLANE STAGNATION POINT FLOW WITH SUCTION

λ_1	λ	K	g	κ_0	κ_{10}	C_0	$\frac{8^*}{\delta}$	$\delta \sqrt{\frac{u_1}{v}}$	$8^* \sqrt{\frac{u_1}{v}}$	$\delta_1 \sqrt{\frac{u_1}{v}}$	$\frac{\tau_0}{\rho U \sqrt{u_1 v}}$
0	0.355	-0.645	0.447	0.0709	0	0	2.37	0.266	0.631	0.595	1.163
.2	.262	-.600	.452	.0536	.0904	.390	2.33	.232	.540	.513	1.39
.4	.177	-.530	.459	.0372	.184	.953	2.28	.193	.440	.420	1.78
.5	.139	-.473	.463	.0299	.231	1.345	2.25	.173	.389	.374	2.07
.6	.100	-.420	.468	.0219	.281	1.900	2.22	.148	.329	.316	2.53
.7	.069	-.346	.474	.0155	.332	2.67	2.18	.125	.271	.264	3.16
.8	.042	-.256	.481	.0098	.385	3.89	2.12	.099	.210	.206	4.26
1.0	0	0	.500	0	.500	∞	2	0	0	0	∞

TABLE 5

THE BOUNDARY-LAYER PARAMETERS AT THE PLANE PLATE
 IN LONGITUDINAL FLOW WITH HOMOGENEOUS SUCTION;
 LENGTH OF GROWING BOUNDARY LAYER

ξ	λ_1	$-K$	$\frac{\delta^*}{\delta_1}$	$\frac{\delta^*}{\theta}$	$\frac{-v_0 \delta^*}{v}$	$\frac{\tau_0 \delta^*}{\mu U_0}$	$\frac{\tau_0}{-\rho v_0 U_0}$	$\sqrt{\xi}$
0	0	1	1.090	2.66	0	0.572	∞	0
0.000171	.02	.989	1.089	2.65	.0218	.576	26.43	.0131
.000662	.04	.979	1.088	2.64	.0435	.581	13.34	.0257
.00154	.06	.968	1.087	2.63	.0652	.586	8.98	.0392
.00291	.08	.956	1.086	2.62	.0869	.591	6.80	.0540
.00456	.10	.945	1.085	2.61	.1085	.597	5.50	.0676
.01139	.15	.916	1.083	2.58	.1624	.610	3.76	.1068
.02037	.20	.884	1.080	2.55	.2159	.625	2.89	.1426
.0341	.25	.851	1.077	2.53	.2692	.640	2.38	.1845
.0517	.30	.817	1.074	2.50	.3221	.656	2.04	.227
.0783	.35	.780	1.070	2.47	.3746	.673	1.80	.280
.1124	.40	.741	1.067	2.44	.4267	.690	1.617	.335
.1551	.45	.700	1.063	2.41	.4784	.707	1.481	.394
.2127	.50	.656	1.059	2.37	.5296	.728	1.375	.461
.2879	.55	.610	1.055	2.34	.5802	.749	1.290	.536
.3883	.60	.560	1.050	2.31	.6303	.770	1.222	.624
.5209	.65	.507	1.046	2.27	.6797	.793	1.167	.722
.7091	.70	.450	1.041	2.24	.7284	.817	1.122	.842
.9756	.75	.389	1.035	2.20	.7763	.843	1.086	.988
1.373	.80	.323	1.029	2.16	.8233	.871	1.058	1.172
2.007	.85	.252	1.023	2.12	.8693	.900	1.035	1.416
3.163	.90	.175	1.016	2.08	.9142	.931	1.018	1.780
5.840	.95	.091	1.008	2.04	.9578	.964	1.007	2.415
10.556	.98	.037	1.003	2.02	.9833	.985	1.002	3.250
14.733	.99	.019	1.002	2.01	.9917	.993	1.001	3.835
∞	1.00	0	1	2	1	1	1	∞

TABLE 6

DRAG LAW OF THE PLANE PLATE IN LONGITUDINAL FLOW
WITH HOMOGENEOUS SUCTION

λ_1	$\xi = f(\lambda_1)$	$F(\lambda_1)$	$G(\lambda_1)$
0	0	0	∞
.01	.0000406	.004665	115.02
.02	.0001706	.008883	52.08
.03	.0003682	.012732	34.56
.04	.0006612	.016623	25.14
.06	.001535	.02646	17.29
.08	.002909	.03608	12.40
.10	.00456	.04719	10.35
.15	.01139	.07427	6.528
.20	.02037	.10506	5.159
.25	.03405	.13949	4.096
.30	.05172	.18066	3.493
.35	.07833	.23006	2.937
.40	.1124	.2872	2.556
.45	.1551	.3539	2.281
.50	.2127	.4357	2.048
.55	.2879	.5357	1.861
.60	.3883	.6614	1.704
.65	.5209	.8199	1.574
.70	.7091	1.0347	1.459
.75	.9756	1.3284	1.362
.80	1.3731	1.7538	1.277
.85	2.0075	2.4165	1.204
.90	3.1630	3.6018	1.139
.95	5.8403	6.3098	1.080
.98	10.556	11.043	1.046
.99	14.73	15.23	1.034
.992	16.15	16.64	1.031
.994	18.01	18.51	1.0275
.996	20.69	21.19	1.0241
.997	22.62	23.12	1.0220
.998	25.37	25.87	1.0196
.999	30.11	30.61	1.0166
.9995	34.90	35.40	1.0143
1	∞	∞	1

$$\frac{c_f}{c_{f\infty}} = G(\lambda_1)$$

$$c_{f\infty} = \frac{-v_0}{U_0}$$

TABLE 7

PARAMETERS FOR THE VELOCITY DISTRIBUTION OVER THE LENGTH OF GROWING
 BOUNDARY LAYER FOR THE PLANE PLATE IN LONGITUDINAL FLOW
 WITH HOMOGENEOUS SUCTION (TO FIG. 12)

$\sqrt{\xi}$	λ_1	-K	$\sqrt{\xi}$	λ_1	-K
0	0	1	1.0	0.754	0.384
.1	.143	.919	1.4	.848	.255
.2	.267	.840	1.8	.902	.171
.4	.453	.696	3.0	.973	.053
.6	.590	.573	∞	1	0
.8	.685	.467			

TABLE 8

 RESULTS OF THE BOUNDARY LAYER CALCULATIONS
 FOR THE CIRCULAR CYLINDER WITH SUCTION
(a) $C_o = 0$

ϕ^o	$\frac{s}{R}$	$\frac{s}{R} \sqrt{\frac{U_o R}{v}}$	$\frac{\delta^*}{R} \sqrt{\frac{U_o R}{v}}$	κ	κ_1	λ	λ_1	$-K$
0	0	0.1883	0.442	0.0709	0	0.355	0	0.653
4	.0698	.1884	.443	.0708		.355		.653
8	.1396	.1888	.446	.0705		.353		.657
12	.2094	.1892	.447	.0700		.350		.660
16	.2793	.1897	.448	.0696		.348		.662
20	.349	.1913	.452	.0668		.345		.664
25	.436	.1944	.459	.0685		.343		.665
30	.524	.1985	.469	.0682		.342		.667
35	.611	.2030	.479	.0675		.340		.669
40	.698	.2071	.488	.0657		.333		.673
45	.785	.2128	.502	.0641		.325		.680
50	.873	.2129	.522	.0612		.312		.690
55	.959	.2259	.540	.0585		.300		.703
60	1.047	.2326	.563	.0541		.280		.720
65	1.134	.2438	.591	.0502		.260		.740
70	1.222	.2552	.623	.0446		.232		.770
75	1.309	.2698	.669	.0377		.202		.805
80	1.396	.2881	.726	.0288		.156		.850
85	1.484	.3087	.790	.0166		.094		.905
90	1.571	.3332	.886	0	0		1.000	
95	1.658	.3583	1.010	-.0223		-.141		1.15
100	1.746	.3937	1.240	-.0538		-.420		1.34
S 101.7	1.776	.4062	1.290	-.0682	↓	-.682	↓	1.44

TABLE 8 - Continued

RESULTS OF THE BOUNDARY-LAYER CALCULATIONS - Continued

(b) $C_o = 0.5$

ϕ^o	$\frac{s}{R}$	$\frac{\delta}{R} \sqrt{\frac{U_o R}{v}}$	$\frac{\delta^*}{R} \sqrt{\frac{U_o R}{v}}$	κ	κ_1	λ	λ_1	$-\kappa$	$\frac{\delta^*}{\delta}$
0	0	0.1573	0.3681	0.0495	0.1112	0.240	0.250	0.580	2.34
4	.0698	.1575	.3686	.0495	.1114	.240	.250	.580	
8	.1396	.1587	.3714	.0494	.1122	.240	.250	.580	
12	.2094	.1598	.3739	.0493	.1130	.240	.250	.581	
16	.2793	.1605	.3756	.0492	.1137	.240	.250	.582	
20	.349	.1619	.3788	.0490	.1145	.240	.250	.584	2.342
25	.436	.1634	.3824	.0487	.1155	.238	.252	.585	
30	.524	.1658	.3880	.0482	.1172	.234	.255	.587	
35	.611	.1695	.3966	.0471	.1199	.225	.260	.589	
40	.698	.1726	.404	.0456	.1220	.220	.267	.592	2.343
45	.785	.1766	.413	.0441	.1249	.215	.275	.595	
50	.873	.1821	.426	.0430	.1288	.208	.290	.601	
55	.959	.1871	.440	.0403	.1323	.195	.297	.608	
60	1.047	.1937	.455	.0375	.1370	.185	.305	.615	
65	1.134	.2012	.473	.0331	.1422	.164	.315	.622	2.35
70	1.222	.2097	.495	.0287	.1481	.141	.329	.630	
75	1.309	.2181	.515	.0230	.1542	.115	.350	.640	
80	1.396	.2289	.543	.0170	.1619	.089	.360	.665	2.37
85	1.484	.2470	.593	.0109	.1747	.057	.375	.695	
90	1.571	.2683	.645	0	.1897	0	.410	.735	2.40
95	1.658	.2881	.709	-.0144	.2037	-.075	.462	.781	
100	1.746	.3123	.835	-.0338	.2208	-.185	.525	.884	2.67
105	1.833	.3421	.978	-.0606	.2419	-.415	.610	1.06	
S 106.4	1.854	.3522	1.004	-.0682	.2490	-.452	.625	1.18	2.84

TABLE 8 - Continued

RESULTS OF THE BOUNDARY LAYER CALCULATIONS - Continued

(c) $C_o = 1$

ϕ^o	$\frac{s}{R}$	$\frac{s}{R} \sqrt{\frac{U_o R}{v}}$	$\frac{s^*}{R} \sqrt{\frac{U_o R}{v}}$	κ	κ_1	λ	λ_1	$-\kappa$
0	0	0.1350	0.3071	0.0365	0.1909	0.170	0.415	0.525
4	.0698	.1350	.3071	.0364	.1909	.170	.415	.525
8	.1396	.1351	.3074	.0362	.1911	.170	.415	.525
12	.2094	.1360	.3094	.0362	.1923	.170	.415	.525
16	.2793	.1367	.3109	.0361	.1933	.169	.417	.525
20	.349	.1373	.3124	.0354	.1942	.166	.420	.525
25	.436	.1383	.3146	.0347	.1956	.162	.425	.524
30	.524	.1400	.3178	.0339	.1966	.156	.430	.523
35	.611	.1419	.3221	.0330	.2007	.153	.440	.522
40	.698	.1442	.3273	.0319	.2039	.150	.445	.521
45	.785	.1466	.3328	.0304	.2073	.142	.455	.520
50	.873	.1491	.3385	.0289	.2106	.135	.470	.519
55	.959	.1532	.3478	.0269	.2167	.127	.485	.517
60	1.047	.1595	.3613	.0254	.2256	.122	.495	.515
65	1.134	.1665	.3762	.0234	.2355	.107	.512	.509
70	1.222	.1729	.380	.0205	.2445	.098	.531	.500
75	1.309	.1795	.394	.0167	.2538	.077	.554	.500
80	1.396	.1869	.410	.0121	.2643	.055	.580	.508
85	1.484	.1942	.435	.0066	.2746	.031	.600	.515
90	1.571	.2017	.450	0	.2852	0	.630	.520
95	1.658	.2090	.476	-.0076	.2956	-.040	.668	.535
100	1.746	.2207	.507	-.0169	.3121	-.088	.710	.560
105	1.833	.2291	.539	-.0272	.3240	-.140	.775	.592
110	1.920	.2500	.598	-.0438	.3436	-.225	.825	.680
115	2.008	.2775	.700	-.0651	.3642	-.357	.850	.835
S 115.5	2.016	.2814	.715	-.0682	.3697	-.375	.870	.870

TABLE 8 - Continued

RESULTS OF THE BOUNDARY LAYER CALCULATIONS - Continued

(d) $C_o = 2$

ϕ^o	$\frac{s}{R}$	$\frac{\delta}{R} \sqrt{\frac{U_o R}{v}}$	$\frac{\delta^*}{R} \sqrt{\frac{U_o R}{v}}$	κ	κ_1	λ	λ_1	$-\kappa$
0	0	0.1030	0.2281	0.0212	0.2913	0.090	0.620	0.420
4	.0698	.1030	.2281	.0211	.2913	.090	.620	.420
8	.1396	.1031	.2284	.0210	.2918	.090	.620	.420
12	.2094	.1034	.2290	.0208	.2925	.087	.621	.419
16	.2793	.1039	.2301	.0205	.2939	.083	.623	.418
20	.349	.1044	.2312	.0198	.2953	.079	.625	.416
25	.436	.1050	.2326	.0194	.2970	.075	.628	.414
30	.524	.1055	.2340	.0190	.2984	.073	.632	.412
35	.611	.1068	.2360	.0185	.3021	.071	.638	.410
40	.590	.1078	.2382	.0178	.3049	.069	.645	.405
45	.785	.1091	.2400	.0168	.3086	.068	.654	.399
50	.873	.1106	.2437	.0157	.3128	.066	.665	.394
55	.959	.1123	.2472	.0145	.3176	.064	.677	.388
60	1.047	.1153	.2524	.0133	.3261	.060	.690	.380
65	1.134	.1187	.2580	.0119	.3357	.052	.710	.370
70	1.222	.1217	.2647	.0101	.3442	.045	.735	.360
75	1.309	.1252	.2712	.0081	.3541	.035	.755	.350
80	1.396	.1289	.2795	.0058	.3646	.025	.775	.340
85	1.484	.1334	.2881	.0031	.3773	.012	.795	.325
90	1.571	.1393	.3002	0	.3940	0	.815	.310
95	1.658	.1460	.3132	-.0040	.4129	-.020	.845	.295
100	1.746	.1543	.3290	-.0083	.4364	-.040	.890	.278
105	1.833	.1631	.3464	-.0138	.4613	-.068	.925	.255
110	1.920	.1721	.3660	-.0202	.4868	-.100	.980	.225
115	2.008	.1860	.3891	-.0306	.526	-.140	1.055	.190
120	2.095	.2015	.415	-.0406	.570	-.185	1.190	.120
125	2.183	.2205	.452	-.0557	.635	-.220	1.260	.038
127.5	2.227	.2371	.472	-.0682	.671	-.305	1.305	-.020

TABLE 8 - Concluded

RESULTS OF THE BOUNDARY-LAYER CALCULATIONS - Concluded

(e) Velocity Distribution

Φ°	$\frac{s}{R}$	$\frac{U_m}{U_o}$	$\frac{R}{U_o} \frac{dU_m}{ds}$
0	0	0	2
4	.0698	.140	1.995
8	.1396	.278	1.981
12	.2094	.416	1.956
16	.2793	.551	1.932
20	.349	.684	1.879
25	.436	.845	1.813
30	.524	1	1.732
35	.611	1.147	1.638
40	.698	1.286	1.532
45	.785	1.414	1.414
50	.873	1.532	1.286
55	.959	1.638	1.147
60	1.047	1.732	1
65	1.134	1.813	.845
70	1.222	1.879	.684
75	1.309	1.932	.518
80	1.396	1.970	.347
85	1.484	1.992	.174
90	1.571	2	0

TABLE 9

 RESULTS OF THE BOUNDARY-LAYER CALCULATION FOR THE SYMMETRICAL
 JOUKOWSKY PROFILE J 015 FOR $c_a = 0$
(a) $f_1(0) = 0; C_0 = 0$

ϕ°	$\frac{s}{t}$	$\frac{s}{t} \sqrt{\frac{U_0 t}{v}}$	$\frac{\delta^*}{t} \sqrt{\frac{U_0 t}{v}}$	κ	κ_1	λ	λ_1	$-K$
180	0	0.0370	0.0878	0.0708	0	0.355	0	0.650
177.5	.0493	.0377	.0895	.0697		.349		.653
175	.00986	.0405	.0964	.0674		.335		.661
172.5	.0148	.0438	.1048	.0630		.319		.682
170	.0197	.0485	.1167	.0581		.298		.703
165	.0308	.0605	.1480	.0464		.247		.753
160	.0444	.0755	.1885	.0351		.197		.802
150	.0764	.1109	.284	.0193		.108		.892
140	.1233	.1572	.411	.0053		.030		.964
136	.1445	.1772	.472	0		0		1.000
130	.1775	.2062	.559	-.0089		-.052		1.062
120	.2416	.2608	.742	-.0260		-.172		1.182
110	.3132	.3217	.960	-.0484	↓	-.362		1.367
S 101.9	.377	.3748	1.310	-.0680		-.628	↓	1.637

TABLE 9 - Continued

RESULTS OF THE BOUNDARY-LAYER CALCULATION - Continued

(b) $f_1(0) = 0.5$; $c_0 = 0.0695$

ϕ^o	$\frac{s}{t}$	$\frac{2}{t} \sqrt{\frac{U_0 t}{v}}$	$\frac{\delta^*}{t} \sqrt{\frac{U_0 t}{v}}$	κ	κ_1	λ	λ_1	$-\kappa$
180	0	0.0359	0.0846	0.0667	0.0180	0.335	0.044	0.640
177.5	.00493	.0366	.0867	.0658	.0183	.331	.045	.645
175	.00986	.0391	.0927	.0634	.0196	.322	.046	.654
172.5	.0148	.0430	.1025	.0603	.0215	.307	.047	.674
170	.0197	.0474	.1140	.0556	.0237	.283	.051	.690
165	.0308	.0580	.1416	.0430	.0299	.227	.060	.734
160	.0444	.0737	.1830	.0334	.0368	.180	.074	.773
150	.0764	.1072	.268	.0169	.0540	.100	.110	.833
140	.1233	.1446	.367	.0045	.0720	.024	.154	.867
136	.1445	.1613	.415	0	.0790	0	.173	.880
130	.1775	.1850	.483	-.0071	.0913	-.035	.203	.906
120	.2416	.2274	.620	-.0200	.1137	-.112	.255	.976
110	.3132	.2793	.764	-.0356	.1397	-.225	.316	1.075
100	.391	.3339	.961	-.0530	.1669	-.360	.384	1.200
S 92.4	.4575	.3742	1.125	-.0682	.1871	-.505	.440	1.310

TABLE 9 - Continued

RESULTS OF THE BOUNDARY-LAYER CALCULATION - Continued

(c) $f_1(0) = 1.0$; $C_0 = 0.139$

ϕ^o	$\frac{s}{t}$	$\frac{\delta}{t} \sqrt{\frac{U_o t}{v}}$	$\frac{\delta^*}{t} \sqrt{\frac{U_o t}{v}}$	κ	κ_1	λ	λ_1	$-\kappa$
180	0	0.0348	0.0819	0.0626	0.0348	0.314	0.077	0.631
177.5	.00493	.0358	.0842	.0626	.0358	.313	.079	.631
175	.00986	.0382	.0900	.0605	.0388	.308	.085	.640
172.5	.0148	.0416	.0985	.0564	.0403	.293	.095	.653
170	.0197	.0460	.1095	.0516	.0450	.265	.104	.667
165	.0308	.0560	.1345	.0376	.0560	.205	.128	.703
160	.0444	.0686	.1678	.0292	.0678	.154	.156	.748
150	.0764	.0985	.243	.0152	.0985	.080	.223	.776
140	.1233	.1342	.332	.0038	.1340	.020	.300	.788
136	.1445	.1484	.368	0	.1478	0	.335	.795
130	.1775	.1682	.421	-.0059	.1682	-.032	.380	.800
120	.2416	.2030	.505	-.0162	.2025	-.084	.465	.806
110	.3132	.2385	.595	-.0270	.2400	-.142	.556	.809
100	.391	.2790	.696	-.0380	.2800	-.200	.650	.812
90	.475	.3200	.800	-.0499	.3203	-.267	.750	.818
80	.561	.362	.916	-.0636	.3622	-.343	.858	.830
S 76.4	.593	.376	.952	-.0682	.3766	-.380	.892	.860

TABLE 9 - Continued

RESULTS OF THE BOUNDARY-LAYER CALCULATION - Continued

(d) $f_1(0) = 1.5$; $C_0 = 0.2085$

ϕ^o	$\frac{s}{t}$	$\frac{s}{t} \sqrt{\frac{U_{ot}}{v}}$	$\frac{s}{t} \sqrt{\frac{U_{ot}}{v}}$	κ	κ_1	λ	λ_1	$-\kappa$
180	0	0.0336	0.0792	0.0584	0.0504	0.295	0.110	0.635
177.5	.00493	.0351	.0824	.0592	.0526	.293	.116	.635
175	.00986	.0372	.0878	.0580	.0557	.281	.125	.639
172.5	.0148	.0404	.0958	.0531	.0606	.265	.136	.648
170	.0197	.0442	.1052	.0482	.0662	.202	.150	.658
165	.0308	.0544	.1301	.0376	.0816	.192	.181	.690
160	.0444	.0675	.1596	.0280	.0980	.145	.220	.705
150	.0764	.0927	.224	.0135	.1391	.070	.310	.722
140	.1233	.1249	.297	.0027	.1852	.016	.415	.718
136	.1445	.1368	.325	0	.205	0	.454	.702
130	.1775	.1543	.365	-.0046	.230	-.014	.512	.669
120	.2416	.1825	.430	-.0127	.272	-.060	.605	.630
110	.3132	.2107	.490	-.0202	.315	-.097	.698	.596
100	.391	.2388	.546	-.0276	.359	-.132	.785	.566
90	.475	.2683	.610	-.0356	.401	-.165	.870	.529
80	.561	.2981	.668	-.0432	.443	-.198	.950	.486
70	.645	.3255	.726	-.0504	.487	-.230	1.034	.430
60	.734	.3555	.770	-.0578	.531	-.260	1.114	.350
50	.807	.3789	.808	-.0637	.568	-.286	1.190	.250
S 40	.885	.4027	.835	-.0682	.604	-.305	1.265	.150

TABLE 9 - Continued

RESULTS OF THE BOUNDARY-LAYER CALCULATION - Continued

$$(e) \quad f_1(0) = 3.0; \quad c_0 = 0.417$$

TABLE 9 - Concluded

RESULTS OF THE BOUNDARY-LAYER CALCULATION - Continued

(f) Velocity Distribution

ϕ°	$\frac{s}{t}$	$\frac{U}{U_\infty}$	$\frac{t}{U_\infty} \frac{dU}{ds}$
180	0	0	51.7
177.5	.00493	.231	49.1
175	.00986	.445	42.2
172.5	.0148	.632	32.6
170	.0197	.782	24.7
165	.0308	.993	12.69
160	.0444	1.111	6.16
150	.0764	1.233	1.572
140	.1233	1.270	.215
136	.1445	1.271	0
130	.1775	1.267	-.209
120	.2416	1.245	-.387
110	.313	1.212	-.468
100	.391	1.178	-.485
90	.475	1.136	-.487
80	.561	1.095	-.487
70	.645	1.053	-.475
60	.734	1.014	-.458
50	.807	.977	-.442
40	.885	.945	-.420
30	.945	.917	-.416
20	.990	.899	-.414
10	1.018	.889	-.410
0	1.028	.884	-.410

TABLE 10
VELOCITY DISTRIBUTION OVER THE REGION OF GROWING BOUNDARY LAYER
FOR THE PLATE WITH HOMOGENEOUS SUCTION

$\sqrt{\xi} = 0.1$		$\sqrt{\xi} = 0.2$		$\sqrt{\xi} = 0.4$		$\sqrt{\xi} = 0.6$		$\sqrt{\xi} = 0.8$	
$\frac{-v_{\infty} y}{v}$	$\frac{u}{U_0}$								
0	0	0	0	0	0	0	0	0	0
.0286	.1108	.0534	.1168	.0910	.1279	.1180	.1373	.137	.1455
.0572	.2176	.1068	.2271	.1820	.2448	.236	.2598	.274	.2727
.0858	.3205	.1602	.3317	.273	.3522	.354	.3697	.411	.3848
.1144	.4173	.2136	.4287	.364	.4497	.472	.4676	.548	.4830
.143	.5107	.267	.5211	.455	.5302	.590	.5584	.685	.5704
.1716	.5967	.3204	.6054	.546	.6215	.708	.6351	.822	.6469
.2002	.6760	.3738	.6826	.637	.6948	.826	.7051	.959	.7141
.2288	.7475	.4272	.7518	.728	.7598	.944	.7666	1.096	.7724
.2574	.8105	.4806	.8126	.819	.8164	1.062	.8196	1.233	.8224
.286	.8663	.5340	.8661	.910	.8659	1.180	.8657	1.370	.8655
.3146	.9112	.5874	.9094	1.001	.9059	1.298	.9029	1.507	.9004
.3432	.9475	.6408	.9442	1.092	.9382	1.416	.9331	1.644	.9287
.3718	.9738	.6942	.9697	1.183	.9621	1.534	.9557	1.781	.9501
.4004	.9899	.7476	.9856	1.274	.9776	1.652	.9708	1.918	.9650
.4290	.9959	.8010	.9920	1.365	.9848	1.770	.9787	2.055	.9734
.5005	.9975	.9345	.9952	1.5925	.9908	2.065	.9871	2.3975	.9839
.5720	.9985	1.0680	.9971	1.820	.9944	2.360	.9922	2.740	.9902
.6435	.9991	1.2015	.9982	2.0475	.9966	2.655	.9953	3.0825	.9941
.715	.9995	1.3350	.9989	2.275	.9980	2.950	.9971	3.425	.9964
.858	.9998	1.6020	.9996	2.730	.9992	3.540	.9989	4.11	.9987
1.001	.9999	1.8690	.9999	3.185	.9997	4.130	.9996	4.795	.9995
∞	1.0000								
$\sqrt{\xi} = 1.0$		$\sqrt{\xi} = 1.4$		$\sqrt{\xi} = 1.8$		$\sqrt{\xi} = 3.0$		$\sqrt{\xi} = \infty$	
$\frac{-v_{\infty} y}{v}$	$\frac{u}{U_0}$								
0	0	0	0	0	0	0	0	0	0
.1508	.1518	.1696	.1617	.1804	.1682	.1946	.1772	.2	.1813
.3016	.2829	.3392	.2986	.3608	.3088	.3892	.3232	.4	.3297
.4524	.3966	.5088	.4149	.5412	.4269	.5838	.4437	.6	.4512
.6032	.4950	.6784	.5137	.7216	.5259	.7784	.5430	.8	.5507
.7540	.5814	.848	.5984	.902	.6095	.973	.6251	1.0	.6321
.9048	.6562	1.0176	.6704	1.0824	.6798	1.1676	.6929	1.2	.6988
1.0556	.7211	1.1872	.7319	1.2628	.7390	1.3622	.7489	1.4	.7534
1.2064	.7770	1.3568	.7840	1.4432	.7887	1.5568	.7952	1.6	.7981
1.3572	.8246	1.5264	.8280	1.6236	.8302	1.7514	.8333	1.8	.8347
1.5080	.8654	1.696	.8651	1.804	.8650	1.946	.8618	2.0	.8647
1.6588	.8984	1.8656	.8953	1.9844	.8933	2.1406	.8905	2.2	.8892
1.8096	.9253	2.0352	.9199	2.1648	.9164	2.3352	.9115	2.4	.9093
1.9604	.9458	2.2048	.9391	2.3452	.9347	2.5292	.9285	2.6	.9257
2.1112	.9614	2.3744	.9533	2.5256	.9486	2.7244	.9421	2.8	.9392
2.262	.9693	2.5440	.9629	2.7060	.9587	2.9190	.9528	3.0	.9502
2.639	.9814	2.968	.9775	3.1570	.9750	3.4055	.9714	3.5	.9698
3.016	.9887	3.392	.9864	3.608	.9848	3.8920	.9827	4.0	.9817
3.393	.9932	3.816	.9917	4.059	.9908	4.3785	.9895	4.5	.9889
3.770	.9959	4.240	.9950	4.510	.9944	4.865	.9931	5.0	.9933
4.524	.9985	5.088	.9981	5.412	.9979	5.838	.9976	6.0	.9975
5.278	.9994	5.936	.9993	6.314	.9993	6.811	.9992	7.0	.9991
∞	1.0000								

The parameter K and λ_1 (See table 7.)

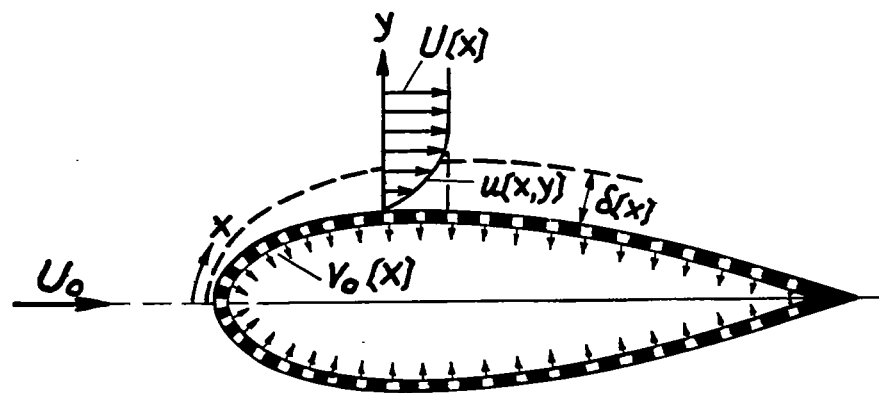


Figure 1.- Explanatory sketch for the boundary layer with suction for arbitrary body shape.

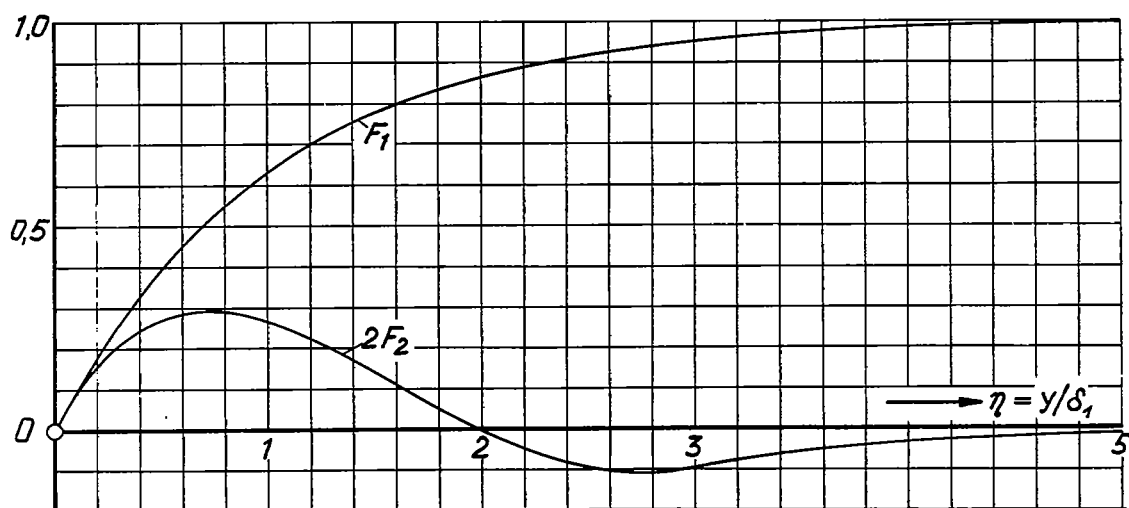


Figure 2.- The functions F_1 and F_2 for the velocity distribution in boundary layer, see equation (9).

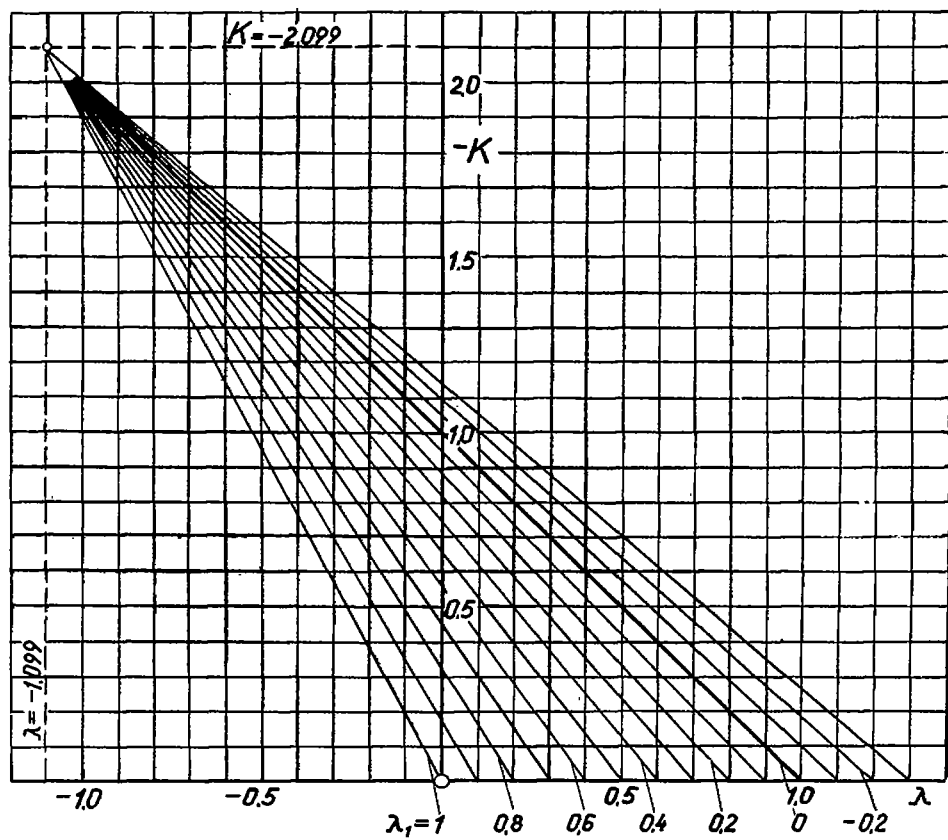


Figure 3.- The form parameter K of the velocity profile as a function of λ , λ_1 , according to equation (14).

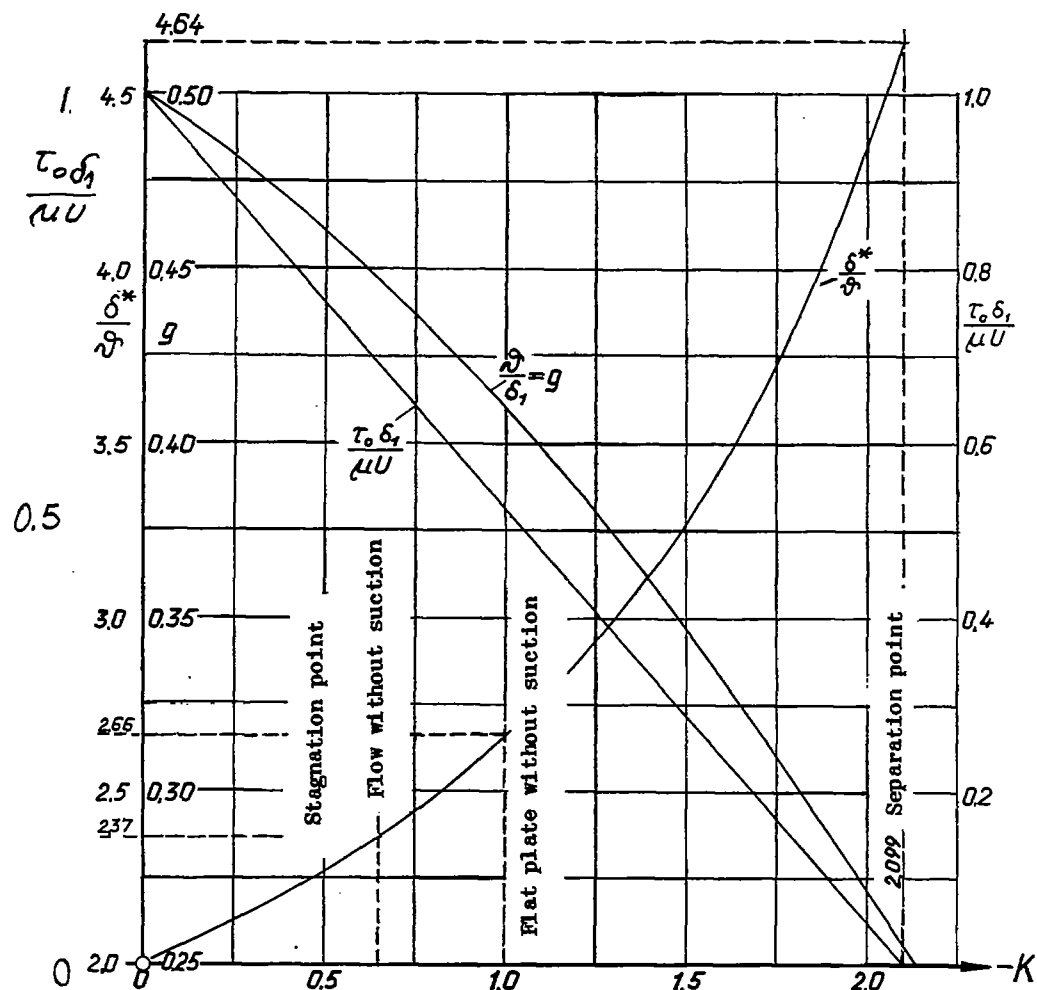


Figure 4. The auxiliary functions $G(K)$, $\frac{\delta^*}{g}$, and $\frac{\tau_0 \delta_1}{\mu U}$ as functions of K , according to equations (17a), (19), and (20).

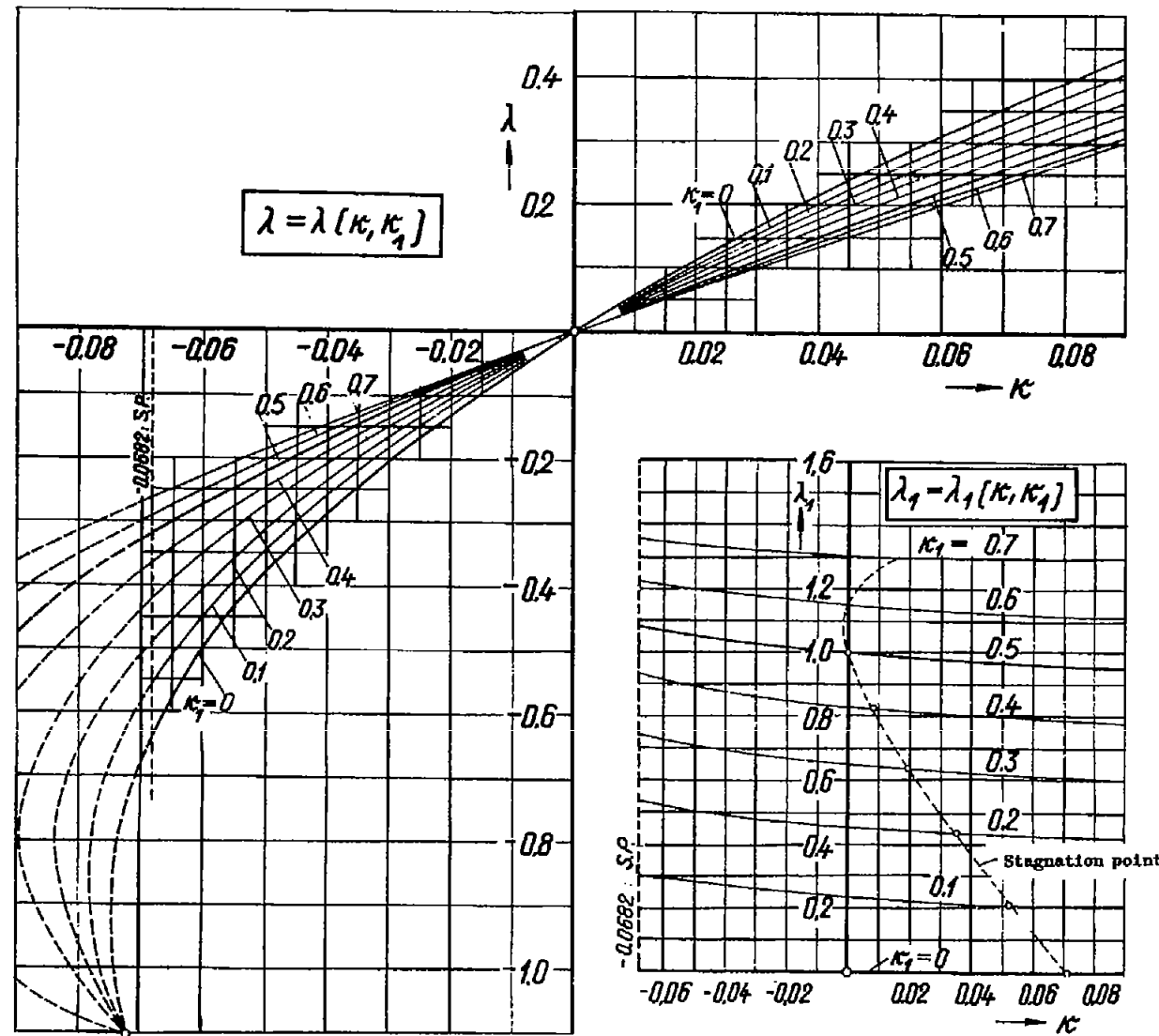


Figure 5.- The parameters λ and λ_1 as functions of κ and κ_1 according to equation (31).

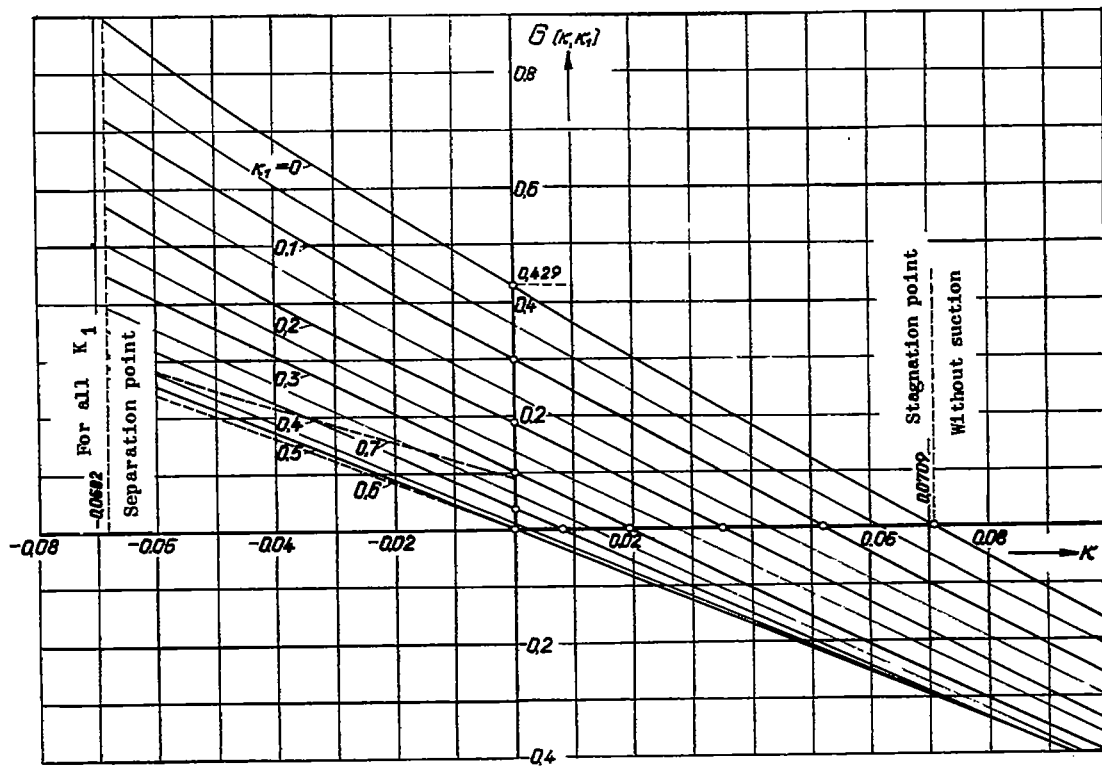
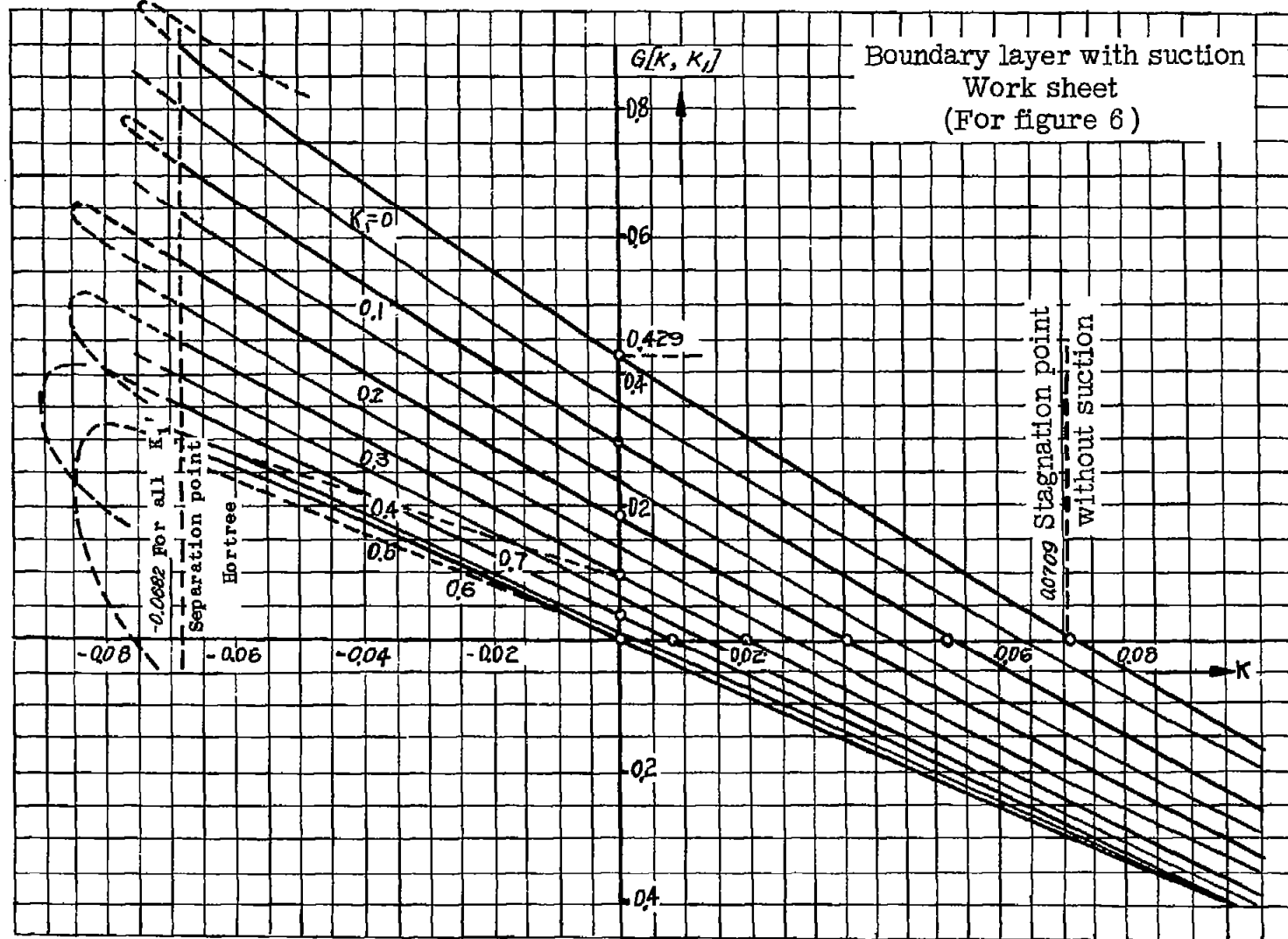


Figure 6.- Diagram for solution of the differential equation for the momentum thickness: $G(\kappa, \kappa_1)$.



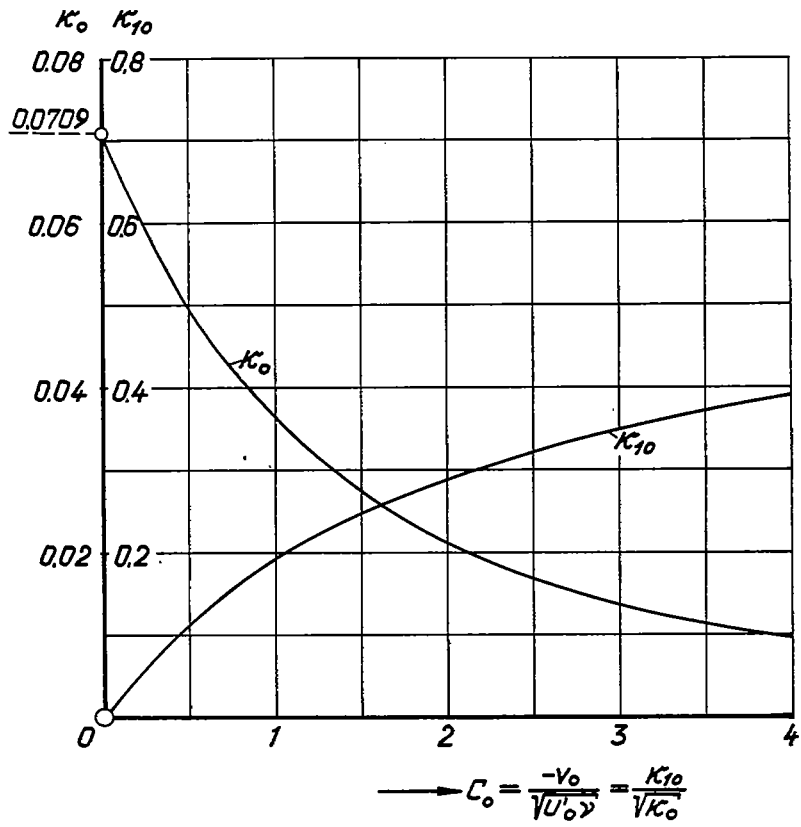


Figure 7.- The initial values of the boundary layer at the stagnation point for various suction quantities.

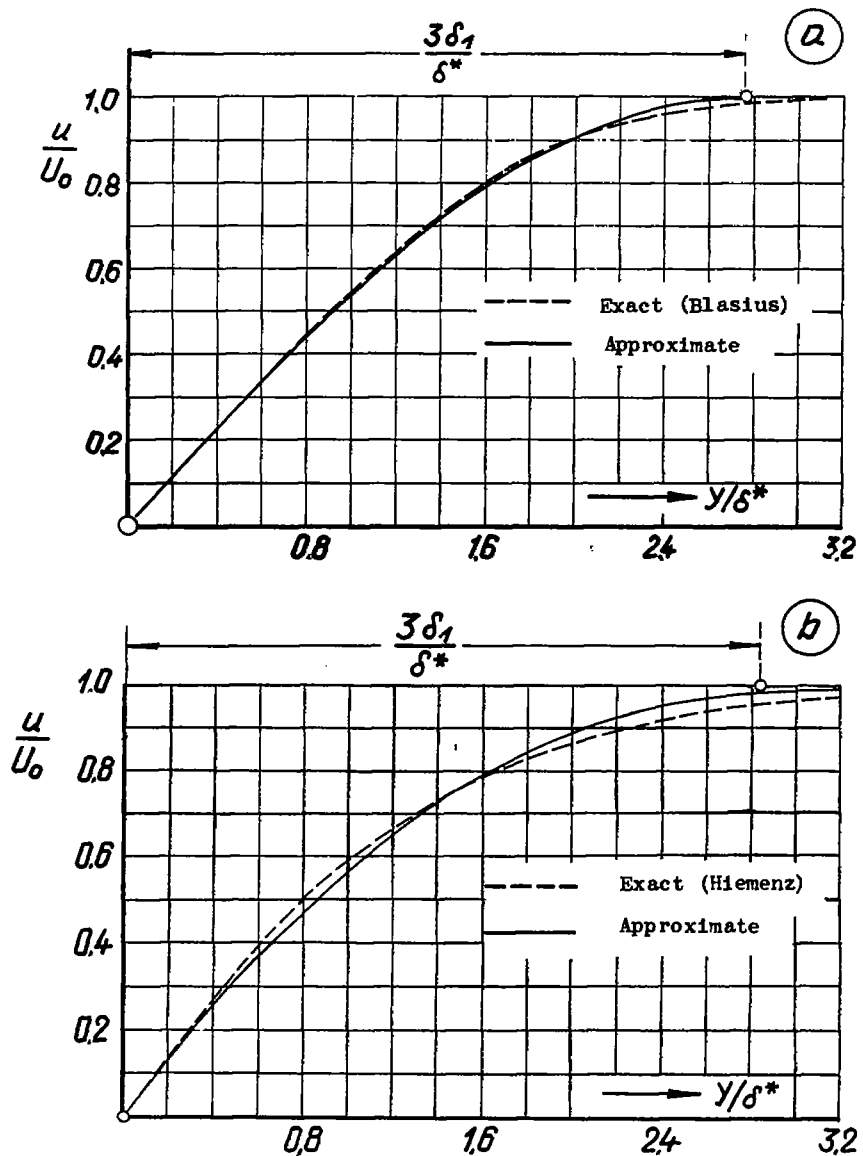


Figure 8.- Comparison of the velocity distributions according to the approximate with the exact calculation.

- (a) Plane plate in longitudinal flow, exact calculation according to Blasius, approximate calculation according to equations (53) and (54).
- (b) Exact calculation according to Hiemenz, approximate calculation according to equations (58) and (58a).

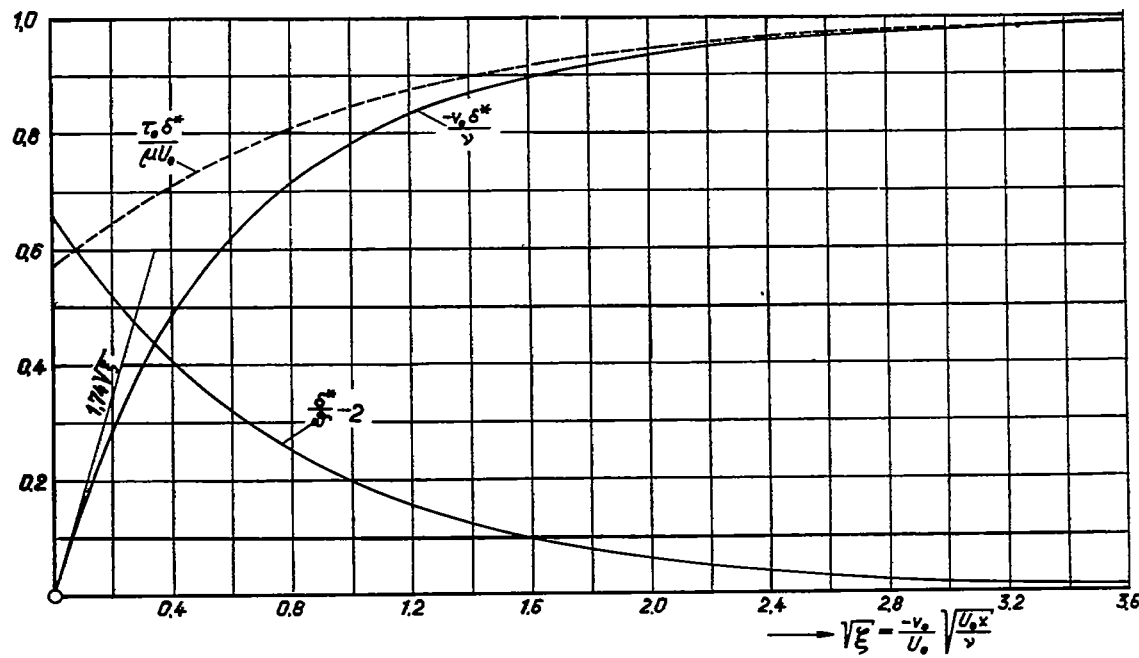


Figure 9.- The extent of growing boundary layer for the plane plate with homogeneous suction: $\frac{-v_0 \delta^*}{\nu}$, $\frac{\delta^*}{\delta}$, $\frac{\tau_0 \delta^*}{\mu U_0}$ against $\sqrt{\xi}$.

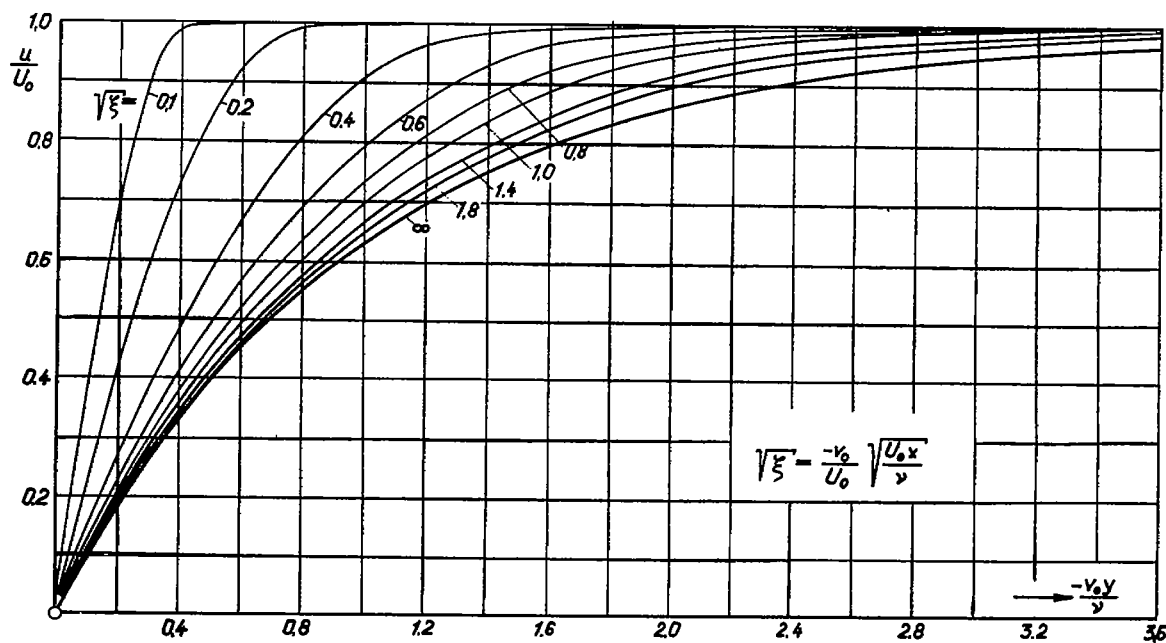


Figure 10.- Plane plate with homogeneous suction; region of growing boundary layer; velocity distribution.

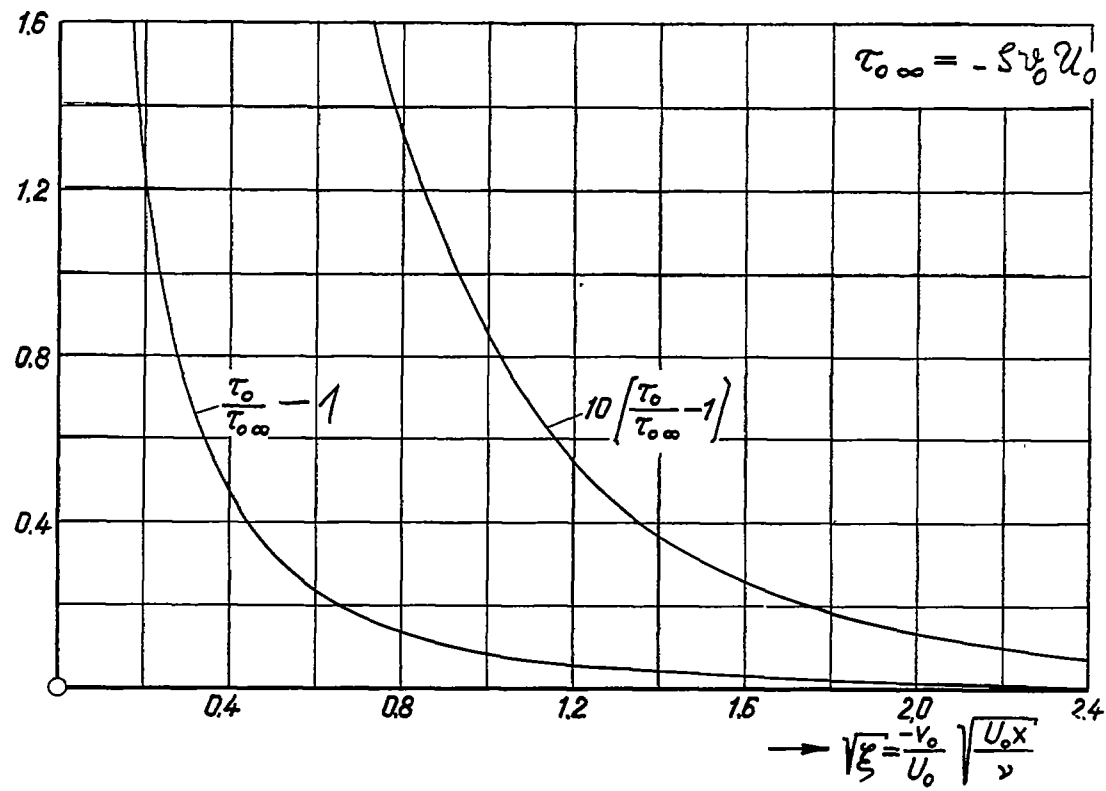


Figure 11.- Plane plate with homogeneous suction; region of growing boundary layer; the local friction coefficient $\frac{\tau_o}{\tau_{o\infty}}$ against $\sqrt{\xi}$.

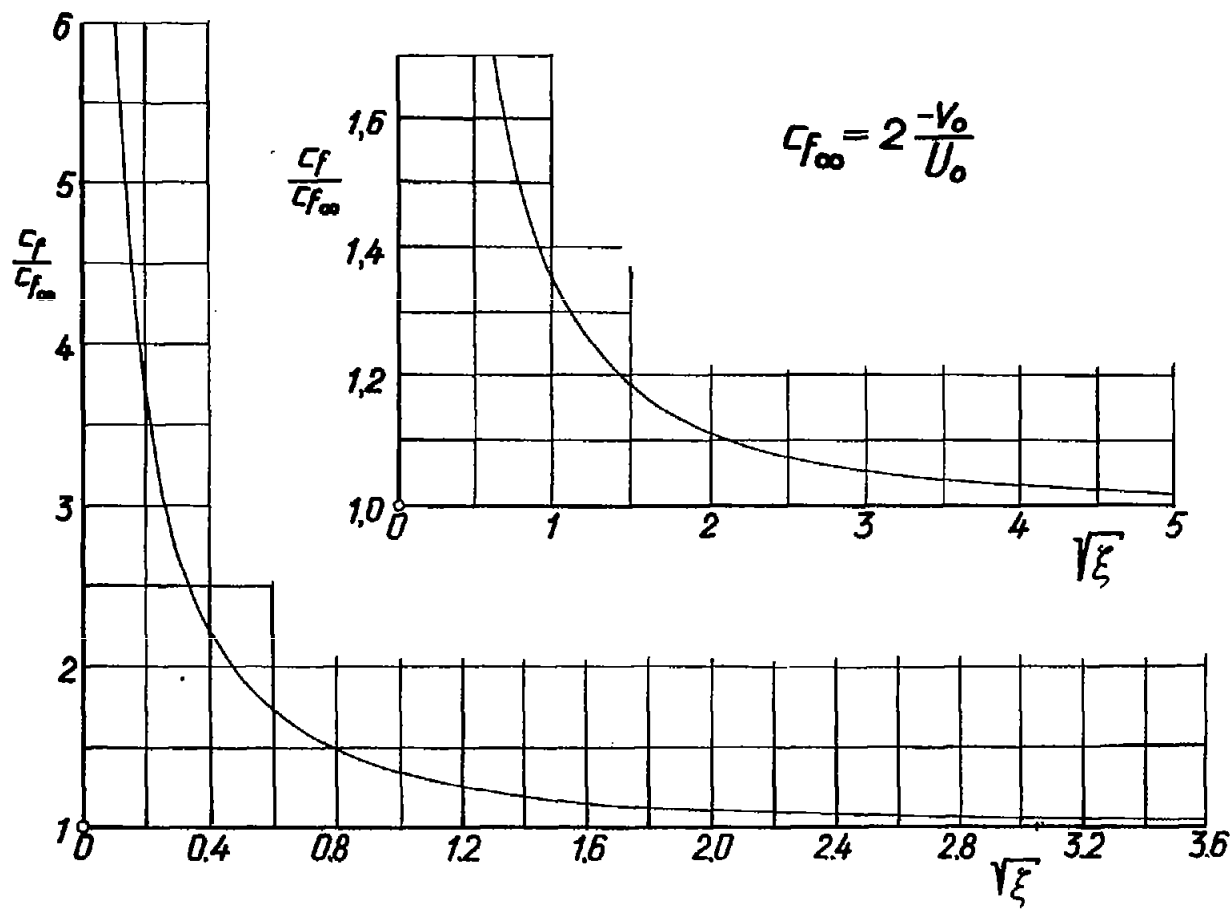


Figure 12.- Plane plate with homogeneous suction, region of growing boundary layer: The coefficient of the

$$\text{total drag } c_f/c_{f_\infty} \text{ against } \sqrt{\xi} = \left(\frac{v_0}{U_0} \right) \sqrt{\frac{U_0 v}{v}} .$$

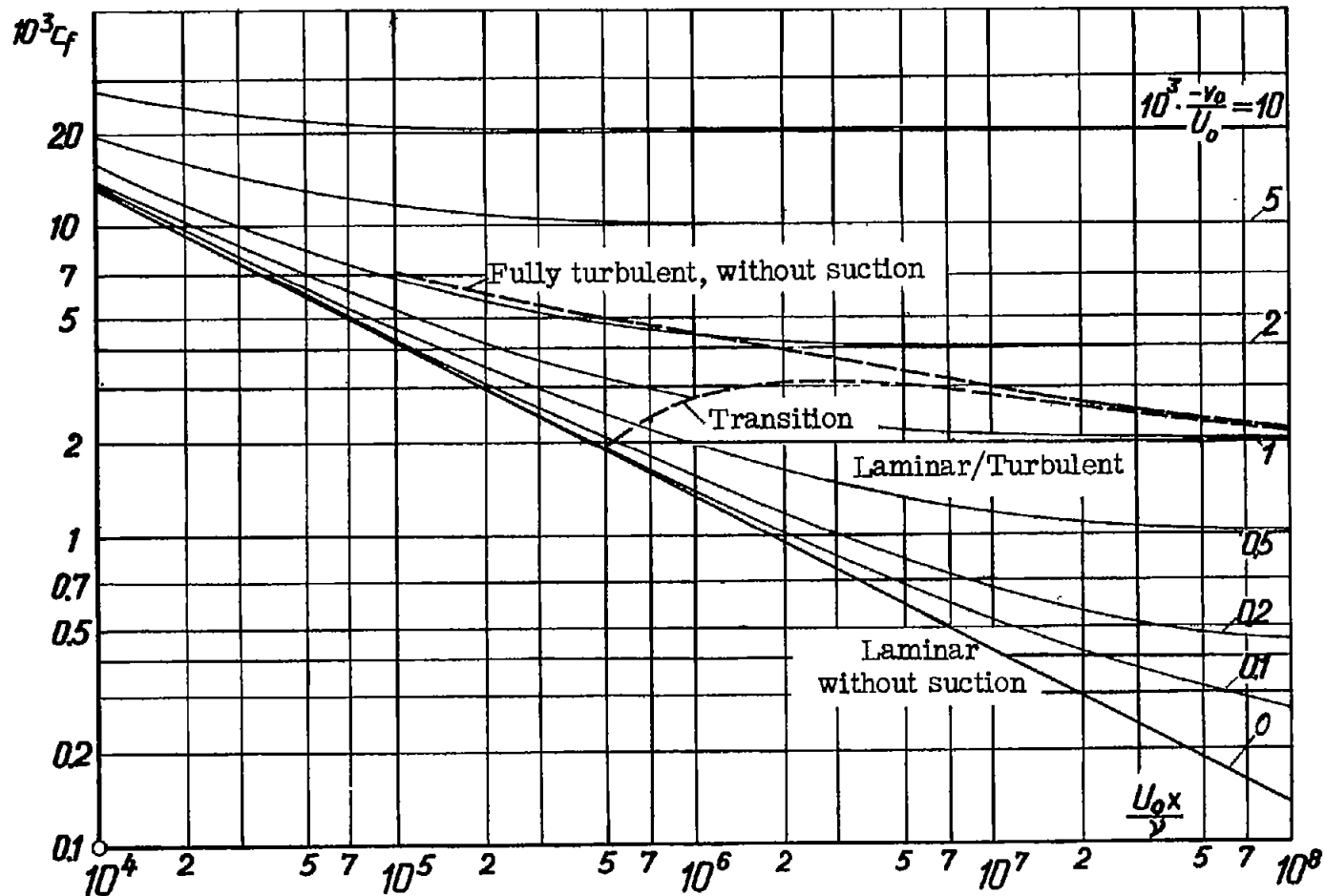


Figure 13.- Plane plate with homogeneous suction, region of growing boundary layer: The coefficient of the total drag c_f against $U_0 l / v$ for various values of suction coefficient $-v_0 / U_0$.

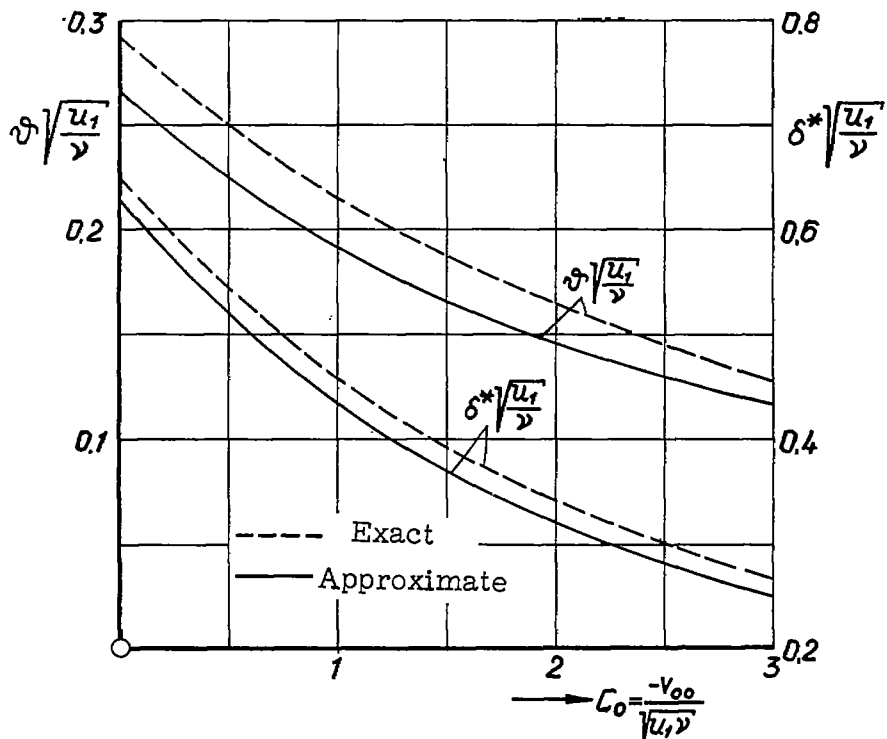


Figure 14.- Plane stagnation point flow: comparison of the boundary-layer thickness and momentum thickness of approximate and exact calculation for various suction quantities, exact calculation according to reference 9.

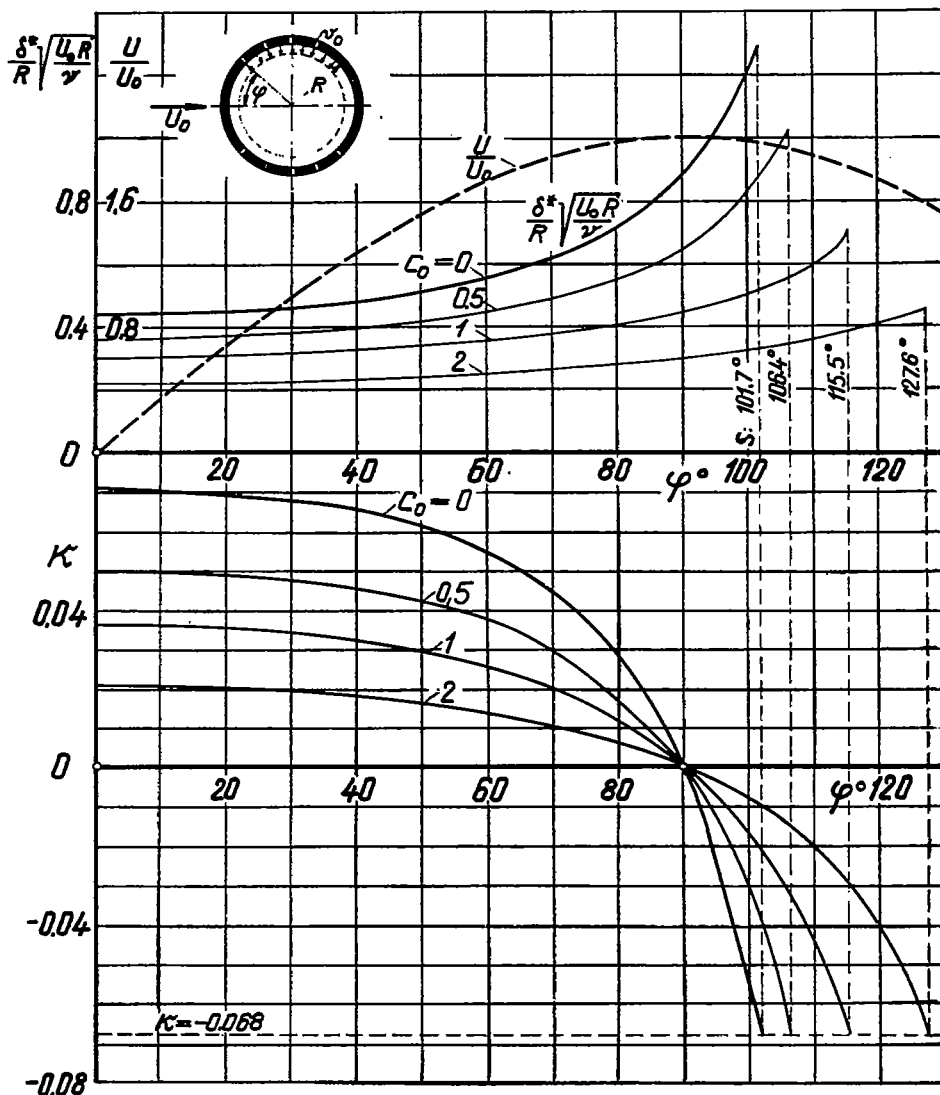


Figure 15.- The boundary layer on the circular cylinder with homogeneous suction for various suction quantities $C_0 = -\frac{v_0}{U_0} \sqrt{\frac{U_0 R}{\nu}}$. Form parameter $\kappa = \frac{\delta^2}{\nu} \frac{dU}{ds}$. With increasing suction quantity the separation point shifts rearward.

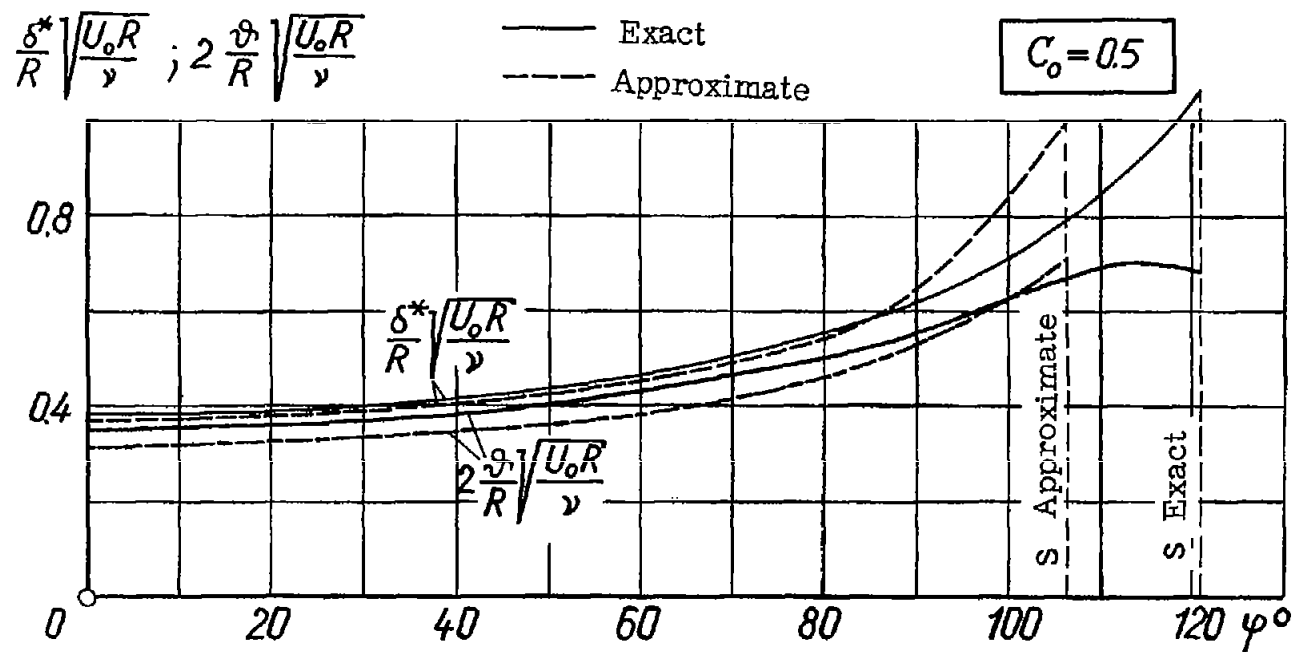


Figure 16.- The boundary layer on the circular cylinder with homogeneous suction for the mass coefficient $C_0 = 0.5$. Comparison of the approximate calculation with an exact solution (reference 17).

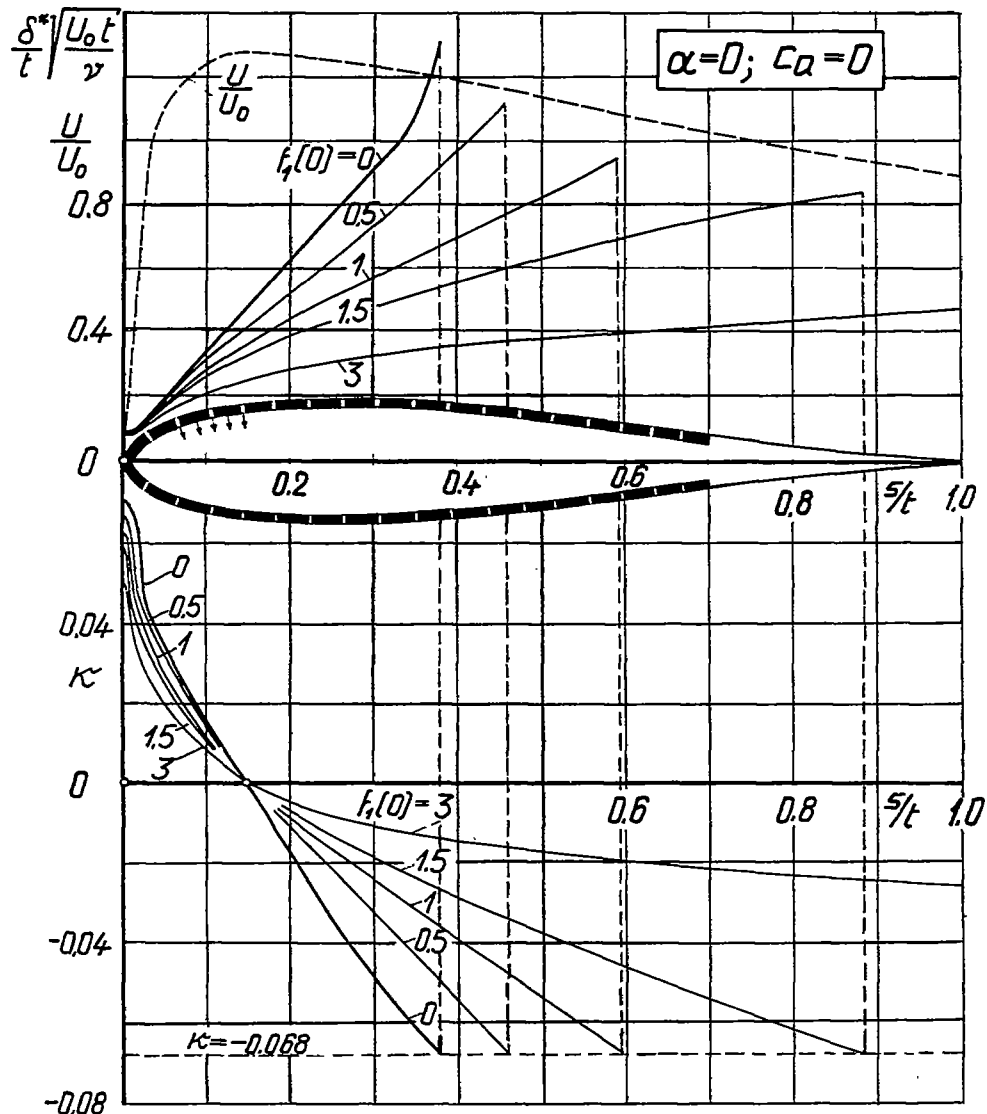


Figure 17.- The boundary layer on a symmetrical Joukowsky profile J 015 with $c_a = 0$ for homogeneous suction with various suction quantities

$$C_o = \frac{f_1(0)}{\sqrt{K_1}} \quad \text{according to equation (36): } C_o = \frac{1}{\sqrt{K_1}} \times f_1(0)$$

$(K_1 = 51.7)$. $\kappa = \frac{v^2}{\nu} \frac{dU}{ds}$. With increasing suction quantity the separation point shifts rearward.

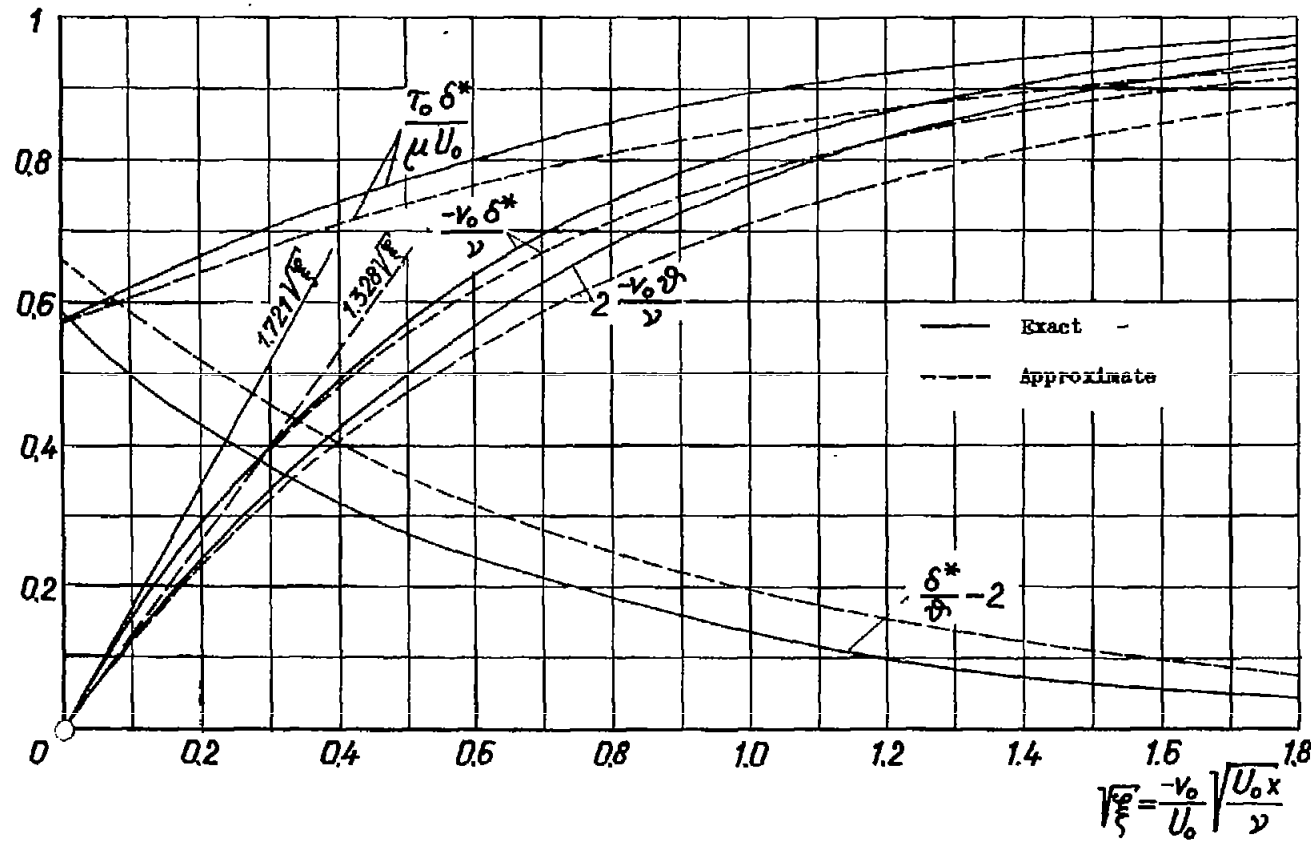


Figure 18.- Region of growing boundary layer for the plane plate with homogeneous suction; comparison of approximate and exact calculation for the displacement and momentum thickness.

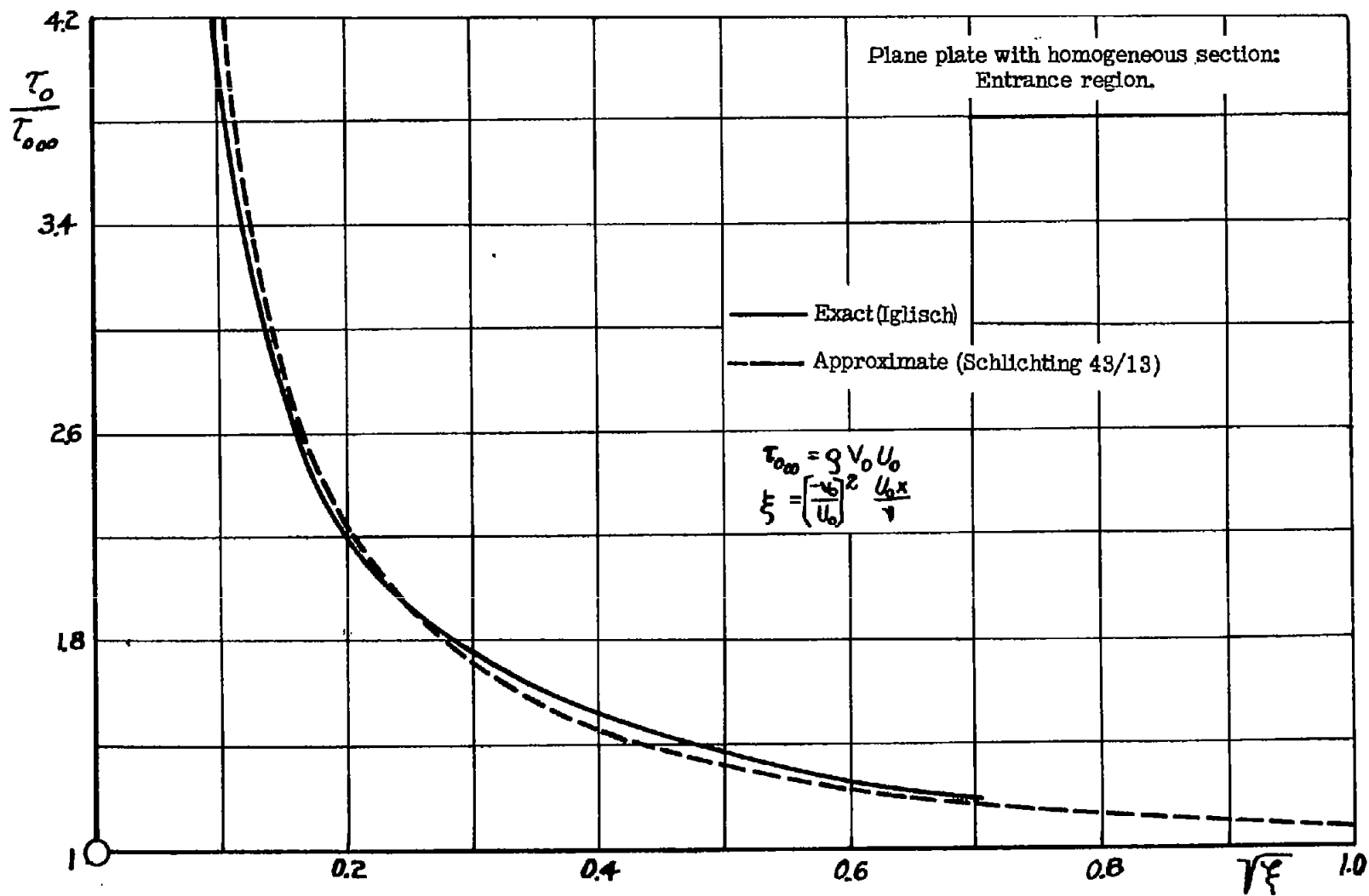


Figure 19.- Region of growing boundary layer for the plane plate with homogeneous suction; comparison of approximate and exact calculation for the wall shearing stress.